TITLE

T cells promote distinct transcriptional programs of cutaneous inflammatory disease in keratinocytes and dermal fibroblasts

AUTHORS

Hannah A. DeBerg[1], Mitch L. Fahning[2], Suraj R. Varkhande[3], James D. Schlenker[4], William P. Schmitt[4], Aayush Gupta[5], Archana Singh[6,7], Iris K. Gratz[2,3,8,9], Jeffrey S. Carlin[10,11], Daniel J. Campbell[2,12], Peter A. Morawski[2,*]

AFFILIATIONS

[1] Center for Systems Immunology, Benaroya Research Institute, Seattle, WA, USA
[2] Center for Fundamental Immunology, Benaroya Research Institute, Seattle, WA, USA
[3] Department of Biosciences and Medical Biology, University of Salzburg, Salzburg, Austria
[4] Plastic and Reconstructive Surgery, Virginia Mason Medical Center, Seattle, WA, USA
[5] Department of Dermatology, Leprology, and Venereology, Dr. D. Y. Patil Medical College, Hospital and Research Centre, Pune, India
[6] Systems Biology Lab, CSIR – Institute of Genomics and Integrative Biology, New Delhi, India
[7] Academy of Scientific and Innovative Research (AcSIR), Gaziabad, India
[8] EB House Austria, Department of Dermatology, University Hospital of the Paracelsus Medical University, Salzburg, Austria
[9] Center for Tumor Biology and Immunology, University of Salzburg, Salzburg, Austria
[10] Center for Translational Immunology, Benaroya Research Institute, Seattle, WA, USA
[11] Division of Rheumatology, Virginia Mason Medical Center, Seattle, WA, USA
[12] Department of Immunology, University of Washington School of Medicine, Seattle, WA, USA
[*] Correspondence: 1201 9th Ave, Seattle, WA 98101, USA; Phone: 1(206)287-1052; E-mail: pmorawski@benaroyaresearch.org

GRAPHICAL ABSTRACT

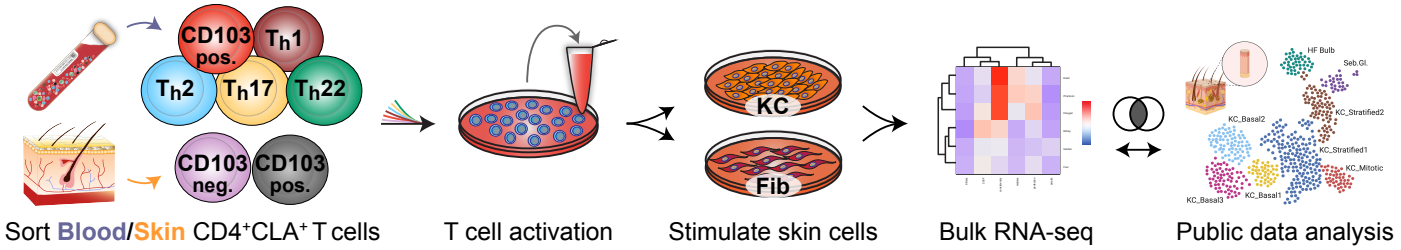

ABSTRACT

T cells and structural cells coordinate appropriate inflammatory responses and restoration of barrier integrity following insult. Dysfunctional T cells precipitate skin pathology occurring alongside altered structural cell frequencies and transcriptional states, but to what extent different T cells promote disease-associated changes remains unclear. We show that functionally diverse circulating and skin-resident $CD4^+CLA^+$ T cell populations promote distinct transcriptional outcomes in human keratinocytes and fibroblasts associated with inflamed or healthy tissue. We identify T_h17 cell-induced genes in keratinocytes that are enriched in psoriasis patient skin and normalized by anti-IL-17 therapy. We also describe a $CD103^+$ skin-resident T cell-induced transcriptional module enriched in healthy controls that is diminished during psoriasis and scleroderma and show that $CD103^+$ T cell frequencies are altered during disease. Interrogating clinical data using immune-dependent transcriptional signatures defines the T cell subsets and genes distinguishing inflamed from healthy skin and allows investigation of heterogeneous patient responses to biologic therapy.

INTRODUCTION

The skin is an immunologically active barrier tissue specialized to deal with a litany of stresses. It contains many immune and structural cell populations whose frequencies, differentiation, and function are altered during inflammatory skin disease. In the epidermis, numerous distinct keratinocyte (KC) and stem cell states have been described by single cell RNA-seq in healthy skin that are altered during psoriasis (Ps) [1]. Transcriptional diversity in the dermis is similarly evident and supported by single cell analyses detailing the gene programs of structural cells such as fibroblasts, pericytes, and endothelial cells [2–5]. One study described the distinct dermal fibroblast (Fib) of healthy subjects and monitored these in individuals with systemic sclerosis (scleroderma; SSc). A progressive loss of LGR5-expressing Fibs (Fib-LGR5), a dominant gene signature in healthy skin, corresponded with SSc severity [3]. Despite the practical advances made in defining the broad transcriptional diversity of skin structural cells, a conceptual framework on how the distinct gene states of skin are regulated during health and disease is lacking.

Functionally specialized skin T cells cooperate with cells of the epidermis and dermis to respond to chemical, biological, and physical stresses [6]. Skin T cells are important in the context of responses to pathogens, allergens, and tumors, in barrier maintenance and wound healing, and they drive disease pathogenesis in many autoimmune and inflammatory diseases. Healthy adult human skin has an average surface area of $1.8m^2$ and contains numerically more T cells than any other non-lymphoid tissue: an estimated 2×10^{10} T cells or ~6% of the total T cell mass in the body [7]. Most skin T cells express cutaneous lymphocyte antigen (CLA), an inducible carbohydrate modification of P-selectin glycoprotein ligand-1 (PSGL-1) and other cell surface glycoproteins [8,9]. CLA-expressing T cells in the blood are a skin-tropic population expressing markers of tissue homing – CCR4, CCR6, CCR8, CCR10 – and make up 5-15% of the circulating $CD4^+$ T cell pool. As with conventional circulating $CD4^+$ T cells, CLA^+ skin-tropic T cells in the blood can be subdivided into distinct helper subsets (T_h) using standard chemokine receptor identification

66 strategies [10]. In addition to traditional T_h subsets, we previously identified $CD4^+CLA^+$ $CD103^+$ T cells, a
67 distinct population of skin resident-memory T cells (T_{RM}) that have the capacity to exit the tissue and form a
68 stable fraction of migratory T_{RM} in the circulation of healthy individuals [11]. We showed that $CD4^+CLA^+$
69 $CD103^{neg}$ and $CD103^+$ skin-resident T cells from healthy donors are transcriptionally, functionally, and
70 clonally distinct populations. Thus, $CD4^+CLA^+$ T cells of the blood and skin include many functionally
71 specialized populations, but how they exert their influence on structural cells of the epidermis and dermis to
72 coordinate skin biology remains incompletely understood.
73 The contribution of T cells and their cytokines is essential to the development of inflammatory skin
74 disease. Accumulation of T cells in lesional tissue and T cell cytokines in patient serum often serve as
75 indicators of active disease, while GWAS have identified polymorphisms in cytokines and cytokine receptors
76 that increase the risk of developing inflammatory skin disease [12–14]. Attempts to target cytokine signaling
77 therapeutically in the skin date back four decades to the use of recombinant IFN in cutaneous T cell
78 lymphoma patients [15]. More recently, IL-17 and IL-23 neutralizing therapies have had immense success at
79 reversing skin pathology during Ps [16,17]. Many candidate therapeutics aimed at altering the abundance or
80 activity of T cell subsets and cytokines are now being used or tested in patients with inflammatory and
81 autoimmune diseases including Ps, atopic dermatitis (AD, eczema), alopecia areata, hidradenitis
82 suppurativa, and SSc [18,19]. While clinical interventions targeting T cell activity during inflammatory skin
83 disease are efficacious, it remains unclear why certain individuals are non-responders to treatment and how
84 functionally specialized cutaneous T cell subsets instruct the structural cell gene programs that distinguish
85 diseased skin from healthy tissue.
86 In this study, we show that subsets of circulating and skin-resident $CD4^+CLA^+$ T cells promote an array
87 of discrete transcriptional outcomes in primary human epithelial KCs and dermal Fibs including the induction
88 of gene programs involved in the inflammatory response, proliferation, barrier integrity, and wound repair.
89 We use this atlas of T cell-dependent effects to investigate gene expression changes occurring during
90 inflammatory skin disease and following intervention in patients receiving anti-cytokine therapy. While some
91 T cell populations potentiate inflammatory responses by KCs and Fibs, others contribute to the maintenance
92 of healthy skin-associated transcriptional programs. These findings inform how T cells contribute to the
93 diverse gene states of skin structural cells, forming the basis for a method to monitor immune-dependent
94 differences between inflamed and healthy tissue and deconvolute patient responses to therapeutic
95 intervention.
96
97 **RESULTS**
98 **<u>Functional characterization of circulating and skin-resident human T cell populations</u>**
99 To assess T cell functional capacity, we isolated 7 distinct blood or skin derived $CD4^+CLA^+$ T_h subsets
100 (*Blood*: T_h1, T_h2, T_h17, T_h22, $CD103^+$; *Skin*: $CD103^{neg}$, $CD103^+$) from healthy controls as described
101 previously [10,11,20] (**Figure 1a, 1b**). Sorted T cell populations were stimulated through the TCR and co-

stimulatory receptors for 48 hours and the production of 13 common T cell cytokines was measured in culture supernatants (**Figure 1c**, **S1**). As expected, T_h cell signature cytokines were enriched: T_h1 (IFNγ), T_h2 (IL-4, IL-5, IL-13), T_h17 (IL-17A, IL-17F), T_h22 (IL-22), CD103$^+$ (IL-13, IL-22). Relative to the blood-derived T cells, those isolated from healthy skin produced lower levels of most measured cytokines (**Figure 1c**). Blood- and skin-derived T cells did both produce comparably high levels of IL-9 (**Figure S1**), a transient

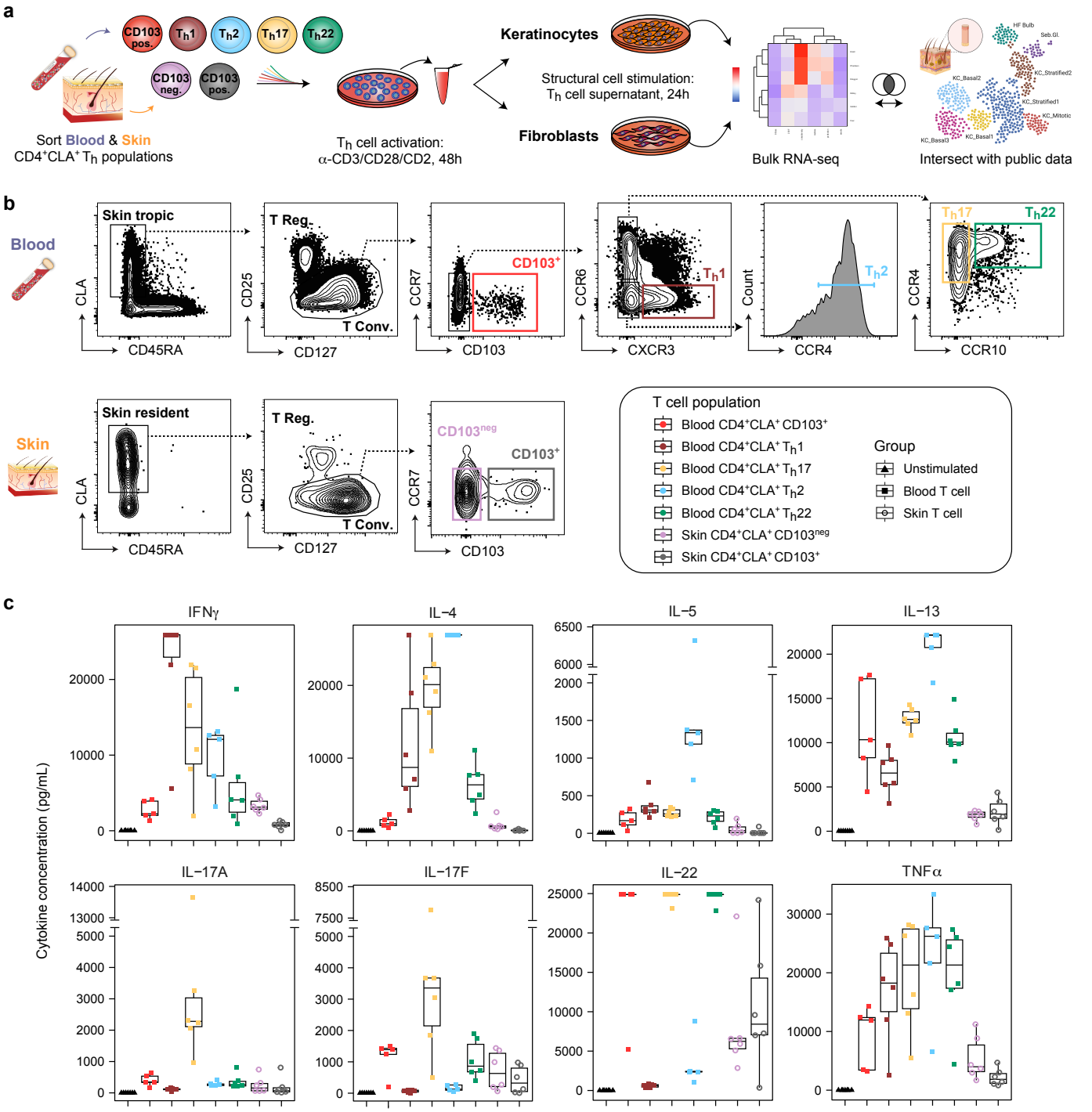

Figure 1. **Isolation and functional characterization of circulating and skin-resident human CD4$^+$CLA$^+$ T cell populations**. (**a**) Experimental design and study schematic: Blood and skin CD4$^+$CLA$^+$ T_h cell isolation, activation, and subsequent stimulation of keratinocytes (KC) and fibroblasts (Fib), analysis by bulk RNA-seq, and comparison to public gene expression data from human skin. (**b**) CD4$^+$CLA$^+$ T_h cell sorting strategy for indicated blood and skin populations. T Conv, conventional T cells; T Reg, regulatory T cells. (**c**) Quantitative cytokine bead array measurement of stimulated T cell supernatants for the 8 indicated analytes (n=5-6 donors per population). Full statistical analysis of cytokine production is provided in **Table S1**.

107 signature cytokine of recently activated CLA^+ T cells [9]. Thus, $CD4^+CLA^+$ T cell populations of both blood and
108 skin produce an array of signature cytokines associated with host defense, tissue repair, and the
109 development of inflammatory skin disease [21].
110

111 **<u>$CD4^+CLA^+$ T cells induce distinct transcriptional states in epithelial keratinocytes and dermal</u>**
112 **<u>fibroblasts</u>**

113 Assessing the effects of individual cytokines on the skin has uncovered specific aspects of tissue biology,
114 but this approach fails to recreate the complexity of an inflammatory response. To determine how each
115 $CD4^+CLA^+$ T_h cell subset impacts the gene expression profile of skin structural cells, we cultured T cell-
116 stimulated supernatants from 5-7 healthy donors per sorted tissue group (blood, skin) together with healthy
117 donor primary KCs or Fibs for 24 hours. The transcriptional response was then assessed by bulk RNA-seq
118 (**Figure 1a**). Unsupervised principal component (PC) analysis revealed that T cell tissue of origin and T_h cell
119 population are the major sources of variance in treated KCs (**Figure 2a, 2b**). Each $CD4^+CLA^+$ T cell
120 population promoted a distinct transcriptional state in the KCs. The top differentially expressed (DE) genes
121 in KCs across all conditions clustered according to both the T cell subset and its tissue of origin (**Figure 2c**).
122 Patterns in T cell-induced gene expression corresponded with the concentrations of cytokines measured in
123 the supernatant of those T cells (IFNγ, IL-4, IL-5, IL-13, IL-17A, IL17F, IL-22, TNFα). A subset of
124 inflammatory response genes known to be induced by T_h1 (i.e. IDO1, CXCL11), T_h2 (i.e. CCL26, IL13RA2),
125 and T_h17 cells (i.e. CSF3, IL23A) also showed expression patterns directly related to the detected amount
126 of IFNγ, IL-4/IL-5/IL-13, or IL-17A/F, respectively (**Figure 2d**). By comparison, skin derived $CD103^+$ T cells
127 and to a lesser extent the migratory $CD103^+$ fraction from the blood drove the expression of genes
128 associated with cell cycle and proliferation in KCs (i.e. MKI67, CDK1).

129 To understand the biological significance of T cell-induced KC transcriptional states, we performed a
130 functional enrichment analysis. Interferon response was largely T_h1 cell-dependent while IL-10
131 immunoregulatory signaling and chemokine receptor pathways were highly enriched in response to T_h17
132 cell supernatants (**Figure 2e, S2a-e**). Skin-derived T cell effects showed enrichment of keratinization and
133 cell cycle pathway genes for $CD103^{neg}$ and $CD103^+$ fractions, respectively (**Figure 2d, 2e, S2f, S2g**). T cell
134 activity broadly altered the baseline cytokine response potential of KCs, as evidenced by dramatic changes
135 in their cytokine receptor expression (**Figure S3**). At rest, KCs constitutively expressed genes required for
136 responsiveness to most T cell cytokines we measured, although CSF2RA (GM-CSF receptor) expression
137 was near the lower limit of detection and neither IL2RA nor IL5R was detected. In response to stimulation,
138 expression of IL10RB and IL22R1 were most highly induced in KCs by T_h1 cells, corresponding to the level
139 of IFNγ measured in stimulated cell supernatants. This is consistent with IFNγ induction of IL-10R as
140 described in gut epithelial cells during barrier restoration [22]. IL17RA and IL17RC expression by KCs,
141 required for IL-17 signaling, were strongly induced by most $CD4^+CLA^+$ T cells tested. Expression of IL2RG,
142 the common gamma chain, was strongly induced in response to stimulation, which potentiates the response

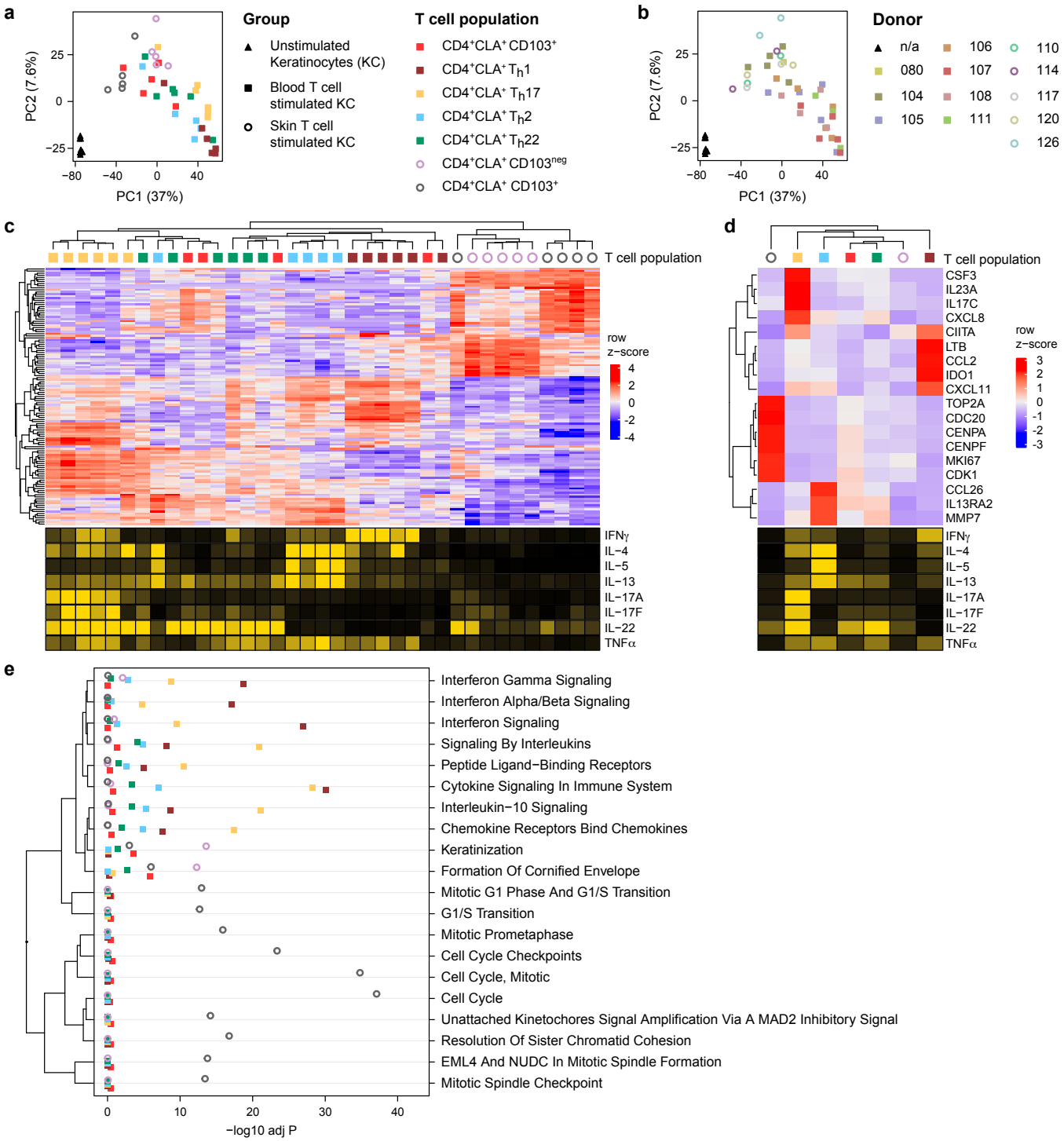

Figure 2. **CD4⁺CLA⁺ T cells induce distinct transcriptional states in epithelial keratinocytes**. (**a**) Principal component (PC) analysis of healthy donor, primary human KCs cultured for 24 hours with the indicated activated blood- or skin-derived T cell supernatants, compared with matched unstimulated controls. (**b**) PC analysis showing each blood (n=7) and skin (n=5) healthy donor-treated KC sample. (**c,d**) *Top*: Heat map showing z-score expression changes of KC genes (*rows*) occurring in response to culture with the indicated donor T cell population supernatant (*columns*). *Bottom*: Heat map showing cytokine production for each donor T cell population, based on quantification in Figure 1. All measures are scaled by quantile. IL-5, IL-17a, and IL-17f are truncated at the 95% quantile due to extreme outliers (c) The top 20 differentially expressed KC genes are shown in response to each indicated donor T cell population. (d) Expression of 18 well-characterized inflammatory and proliferative response elements in KC averaged across all donor samples for each T cell subset. (**e**) Dot plot showing functional enrichment analysis of differentially expressed, T cell-induced KC genes within the indicated modules (n=5-6 donors per population). The -log10 adjusted P value is plotted as a statistical measure for enrichment within each module.

to multiple other cytokines (IL-2, IL-4, IL-7, IL-9, IL-15). In these ways, CD4⁺CLA⁺ T cell subset activity can shape the outcome of cutaneous immune responses.

146 As observed in KCs, stimulation with blood and skin T cell supernatants had a strong effect on the
147 transcriptional response in healthy donor dermal Fibs (**Figure 3a**). The largest effect size comes from T cell
148 tissue of origin – blood versus skin – and while the impact of individual T_h populations was evident, this was
149 less pronounced than that observed in KCs (**Figure 3a-c, S4**). The top DE genes in Fibs were separated
150 into three main blocks: those associated with T_h1 activity and high levels of the pro-inflammatory cytokine
151 IFNγ; those associated with blood-derived T_h cells producing either type 2 or type 17-associated cytokines;
152 and those associated with skin-derived T cells that produced proportionally more IL-22 and IL-9 than other
153 subsets tested (**Figure 3c**). Each T cell population induced a different set of genes, though the main
154 response in Fibs occurred largely downstream of either T_h1/IFNγ or T_h17/IL-17 (**Figure 3d, S4b, S4c**). Cell
155 cycle and proliferation genes were elevated in response to skin-derived T cell supernatants, as observed in
156 KCs, but also by T_h17 and blood $CD103^+$ T cell activity. A pathway analysis of the Fib response revealed
157 broad engagement of cytokine signaling downstream of common $CD4^+$ T cell cytokines including IFNγ, IL-4,
158 IL-13, and IL-10 (**Figure 3e**). Skin $CD103^{neg}$ T cells uniquely promoted metal ion and metallothionein
159 signaling pathways, essential components of wound healing and the fibrotic response [23]. As with KCs,
160 treatment with T cell supernatants substantially altered cytokine receptor expression on Fibs (**Figure S5**).
161 For example, induction of IFNGR1 and IL17RA in Fibs was induced by both blood- and skin-derived
162 $CD4^+CLA^+$ T cells, consistent with our observation that a large part of the dermal Fib response to T cells is
163 dependent on T_h1/IFNγ and T_h17/IL-17 signaling. In contrast, IL13RA2 expression is promoted by T_h2, T_h17,
164 T_h22 and blood $CD103^+$ T cells, which each produce varying amounts of IL-13 and low levels of IFNγ. Once
165 thought to be only a decoy receptor, IL13RA2 is an important mediator of IL-13-dependent fibrotic
166 responses in barrier tissues [24,25]. The baseline expression of IL31RA and OSMR were also elevated in
167 stimulated Fibs, potentiating responsiveness to IL-31, a T cell cytokine involved in pruritis and atopic
168 dermatitis [26,27]. Finally, TGFBR1 and TGFBR2 expression were antagonized by blood- but not skin-derived
169 $CD4^+CLA^+$ T cells. Collectively, these data show that $CD4^+CLA^+$ T cells can induce transcriptionally distinct
170 states in epithelial KCs and dermal Fibs including those associated with inflammatory, regulatory,
171 proliferative, and fibrotic gene programs of the skin.
172

173 **<u>T cell-dependent gene signatures are enriched in the epidermis during inflammatory skin disease</u>**
174 **<u>and normalized by anti-cytokine therapy</u>**

175 Phenotypically and functionally distinct T cell populations accumulate in lesional tissue during inflammatory
176 and autoimmune skin diseases [6,12]. Ps (~3% prevalence in the US) and AD (~7% prevalence in the US) are
177 two common skin inflammatory diseases in which dysregulated T cell activity is central to the development
178 or persistence of tissue pathology [6,28,29]. Ps is primarily associated with elevated T_h17 cell and IL-17
179 responses in the skin, whereas AD is canonically associated with T_h2 cells and IL-13 activity, while IL-4 and
180 IL-5 responses are mostly absent [30,31]. The pathogenic role of T cell-derived cytokines in these diseases is
181 highlighted by the success of biologic therapies: i.e. secukinumab and ixekizumab for Ps (anti-IL-17A);

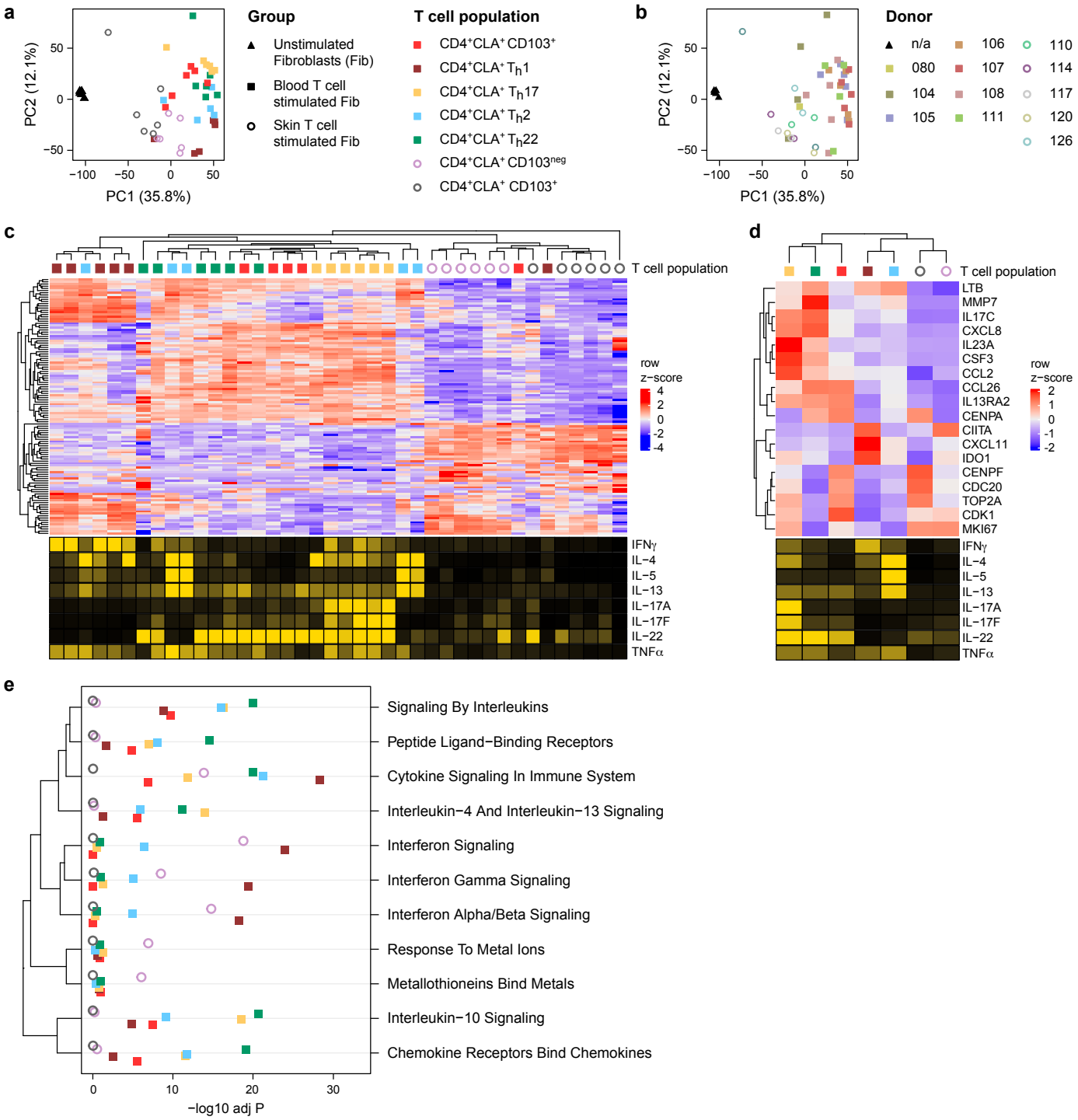

Figure 3. **CD4⁺CLA⁺ T cells induce distinct transcriptional states in dermal fibroblasts**. (**a**) Principal component (PC) analysis of healthy donor, primary human KCs cultured for 24 hours with the indicated activated blood- or skin-derived T cell supernatants, compared with matched unstimulated controls. (**b**) PC analysis showing each blood (n=7) and skin (n=5) healthy donor-treated Fib sample. (**c,d**) *Top*: Heat map showing z-score expression changes of Fib genes (*rows*) occurring in response to culture with the indicated donor T cell population supernatant (*columns*). *Bottom*: Heat map showing cytokine production for each donor T cell population, based on quantification in Figure 1. All measures are scaled by quantile. IL-5, IL-17a, and IL-17f are truncated at the 95% quantile due to extreme outliers. (c) The top 20 differentially expressed Fib genes are shown in response to each donor T cell population. (d) Expression of 18 well-characterized inflammatory and proliferative response elements in Fibs averaged across all donor samples for each T cell subset. (**e**) Dot plot showing functional enrichment analysis of differentially expressed, T cell-induced Fib genes within the indicated modules (n=5-6 donors per population). The -log10 adjusted P value is plotted as a statistical measure for enrichment within each module.

dupilumab and tralokinumab for AD (anti-IL4Rα, anti-IL13) [32–35]. Using the structural cell gene signatures generated in Figures 2 and 3, we assessed the relationships between T cell activity, dysfunctional gene

programs in skin structural cells during inflammatory disease, and patient responses to anti-cytokine therapy. As KCs are the majority population in the epidermis and alongside Fibs are the most abundant cells in human skin [36], we expected an analysis of full thickness skin biopsies would primarily reflect changes in KC and Fib gene programs.

We combined publicly available gene expression data of lesional, non-lesional, and healthy control donor skin from three clinical trials that demonstrated the efficacy of anti-IL-17A therapies in patients with Ps [GSE137218, GSE166388, GSE31652] [37–40], batch correcting to adjust for study-specific effects. The concatenated transcriptomic data sets clustered by disease state and treatment (**Figure 4a, S6a**). DE gene analysis revealed a pre-treatment lesional Ps skin gene expression profile that was altered over the course of anti-cytokine treatment, eventually resembling that of healthy control and non-lesional skin (**Figure 4a, 4b**), reflecting the known efficacy of these drugs.

We next looked for T cell-dependent gene expression changes in Ps patient skin over the course of anti-IL-17A therapy. We found that gene signatures induced by T cell populations in KCs (**Figure 2**) were broadly increased as a part of the dysregulated transcriptional signature of disease (**Figure 4c**). The T_h17-KC gene signature showed both the strongest association with the transcriptional dysregulation measured in Ps lesional skin and the subsequent response to therapy, compared to other T-dependent effects measured (**Figure 4d**). By day 84, both T_h17-KC and T_h22-KC signatures were significantly decreased in patient skin in response to therapy relative to day 0 lesional skin, consistent with the known role of IL-17 producing $CD4^+$ T cells in Ps (**Figure 4c, 4d**). Of the 93 unique T_h17-induced KC signature genes we identified (**Figure S2c**), 24 (26%) were DE between Ps and healthy skin samples. Of these 24 genes, 13 (54%) were significantly responsive to anti-IL-17A therapy while 11 (46%) were not (**Figure S6b**). We next assessed individual T cell-KC signature genes in lesional Ps skin compared either to healthy control or anti-IL-17A treated samples and found that many of the significant differences were T_h17 cell-induced, disease-associated, and responsive to therapy (**Figure 4e**).

Further investigation revealed T_h17-dependent KC genes that have Ps-associated GWAS SNPs near their transcriptional start site (TSS) (**Figure 4f**). The risk allele *rs7556897* is located 10.3kb from the CCL20 gene [41]. It has a high variant-to-gene (V2G) score and impacts CCL20 as shown by expression and protein quantitative trait locus (eQTL, pQTL) mapping studies [42–44]. Another, *rs9889296*, is located 75.9kb from CCL8 and is implicated by fine mapping as an eQTL [41,45]. IL19 has 3 reported Ps GWAS hits: *rs3024493*, an eQTL for IL19 located 141bp from the TSS [41]; *rs55705316*, located 10.6kb from the TSS with Hi-C data showing promoter proximity; [46,47] *rs12075255*, 17.5kb from TSS [41]. CCL20 and CCL8 coordinate immune cell recruitment to the tissue [48] while IL19 is a part of the IL-17/IL-23 inflammatory axis of Ps and among the most DE cytokines measured between Ps [49]. Our analysis demonstrated that CCL20, CCL8, and IL19 – genes elevated during the Ps epidermal inflammatory response and significantly impacted in response to anti-IL-17A therapy – are each uniquely induced by T_h17-cells in KCs (**Figure 4f**). Published V2G mapping, eQTL and Hi-C studies complement our findings, reinforcing the functional relevance of these T cell-

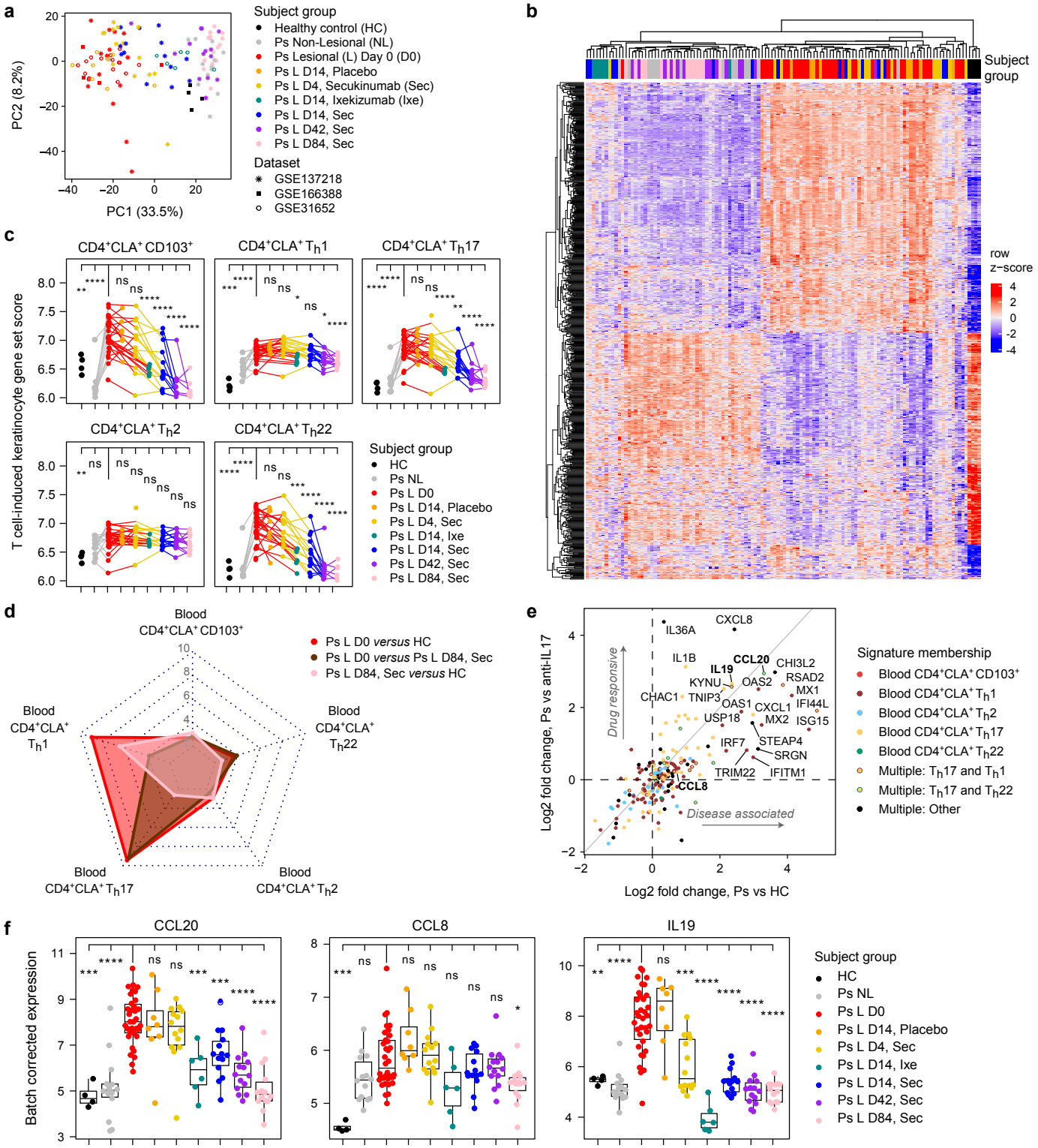

Figure 4. **T cell-dependent gene signatures are enriched in the epidermis during psoriasis and normalized by anti-IL-17A**. (**a**) PC analysis of gene expression for paired donor Ps lesional or non-lesional skin compared with healthy controls (HC) from the indicated public data sets. Subjects were treated with an anti-IL-17A therapy – secukinumab (Sec), ixekizumab (Ixe) – or placebo. Merged data sets were batch corrected to adjust for study-specific effects. (**b**) Heat map showing z-score expression changes of KC genes determined to be T cell-dependent (Figure 2) within public data, as shown in 'a' for the indicated groups. (**c**) Plots showing blood T cell-induced gene set scores, an averaged measure for the effect of each T cell subset on healthy donor KCs per subject group. (**d**) Radar plot showing T cell-induced KC signature gene enrichment values for the indicated pairwise comparisons from public data with -log10 p-values plotted along the radial axis. (**e**) Bivariate plot of the log2 fold change between subject groups for T cell-dependent KC genes (Ps vs HC, 'Disease associated'; Ps vs anti-IL17A, 'Drug responsive'). Individual genes are colored according to their T cell signature membership. (**f**) Plots showing batch corrected gene expression for each subject group for genes that have at least one expression-modulating Ps-associated SNP (i.e. eQTL). All statistical measures shown are compared to the Ps Lesional D0 group. Error bars indicate mean ± SD; ns = not significant, *p ≤ 0.05, **p ≤ 0.01, ***p ≤ 0.001, and ****p ≤ 0.0001 (Student's *t*-test).

222 dependent target genes during Ps.

223 Not all the T-dependent KC genes we observed in lesional Ps skin were significantly impacted by anti-
224 IL-17A therapy. Two examples are CXCL2, a neutrophil recruitment factor described to be part of the
225 inflammatory axis of Ps [50], and NES, a gene encoding the intermediate filament nestin, which is expressed
226 in skin epidermal stem cells and posited to be important during epithelial cell proliferation (**Figure S6b**) [51].
227 CXCL2 and NES along with 9 other T_h17-dependent genes are Ps-associated, but their expression is not
228 significantly altered by anti-IL-17A blockade. Thus, we were able to discern a mixed effect of cytokine
229 blockade on T cell-dependent gene expression in the skin, though it remains unclear which of these genes
230 are central indicators of patient outcome to therapy.

231 We took a similar approach to analyze publicly available skin RNA-seq data from an AD clinical trial that
232 tested the efficacy of IL-4R blockade by dupilumab [GSE157194] [52] and from matched AD patients and
233 controls [GSE121212] [53]. Most of the variance in the combined data set could be explained by disease
234 state, while a smaller effect was evident in response to treatment (**Figure 5a, S7a**). We focused our
235 analysis on DE genes that we identified as T cell-dependent in KCs (**Figure 2**). Using this strategy, the data
236 separated largely by tissue type; lesional, non-lesional, and healthy skin. Samples in dupilumab treated
237 groups were dispersed throughout hierarchical clusters, indicating a mild treatment effect on total T cell-
238 dependent KC genes (**Figure 5b**). When comparing subset-specific T cell-KC gene expression across all
239 subject groups we found a significant effect of dupilumab on the expression of $CD4^+CLA^+$ T_h2, T_h22, and
240 $CD103^+$ T cell-dependent genes within lesional skin (**Figure 5c**). All T cell-KC gene sets were significantly
241 upregulated within lesional skin samples compared with those from healthy skin, an effect that was
242 diminished in response to therapy (**Figure 5c, 5d**). Dupilumab targets IL-4 and IL-13 activity, two cytokines
243 made co-produced in abundance by $CD4^+CLA^+$ T_h2 cells (**Figure 1d**). We identified a set of seven uniquely
244 T_h2-induced KC genes that were significantly elevated in lesional AD skin compared to controls (**Figure 5e,**
245 **S7b**). Of these, CA2, SLC5A5, and SLC26A9 were significantly reduced in lesional skin following dupilumab
246 treatment (**Figure S7c**). CA2 encodes a carbonic anhydrase important for cellular pH and ion homeostasis,
247 previously shown to be elevated in AD patient skin and differentiated KCs [54,55]. SLC5A5 and SLC26A9
248 encode iodine and chloride channel proteins, respectively, and neither have a known role in promoting
249 pathology during AD.

250 Our findings demonstrate that T cell-dependent KC gene networks experimentally derived *in vitro*: (1)
251 are enriched *in vivo* within human skin; (2) are associated with cutaneous inflammatory disease; and (3)
252 some but not all are normalized in response to anti-cytokine biologic therapy. Further disease relevance is
253 highlighted by fine-mapping studies that link GWAS-identified SNPs to the expression of T-dependent
254 genes we describe. Thus, we validate a method of identifying candidate genes to explain immune-
255 dependent effects during inflammatory disease and to deconvolute the patient response to therapy.
256

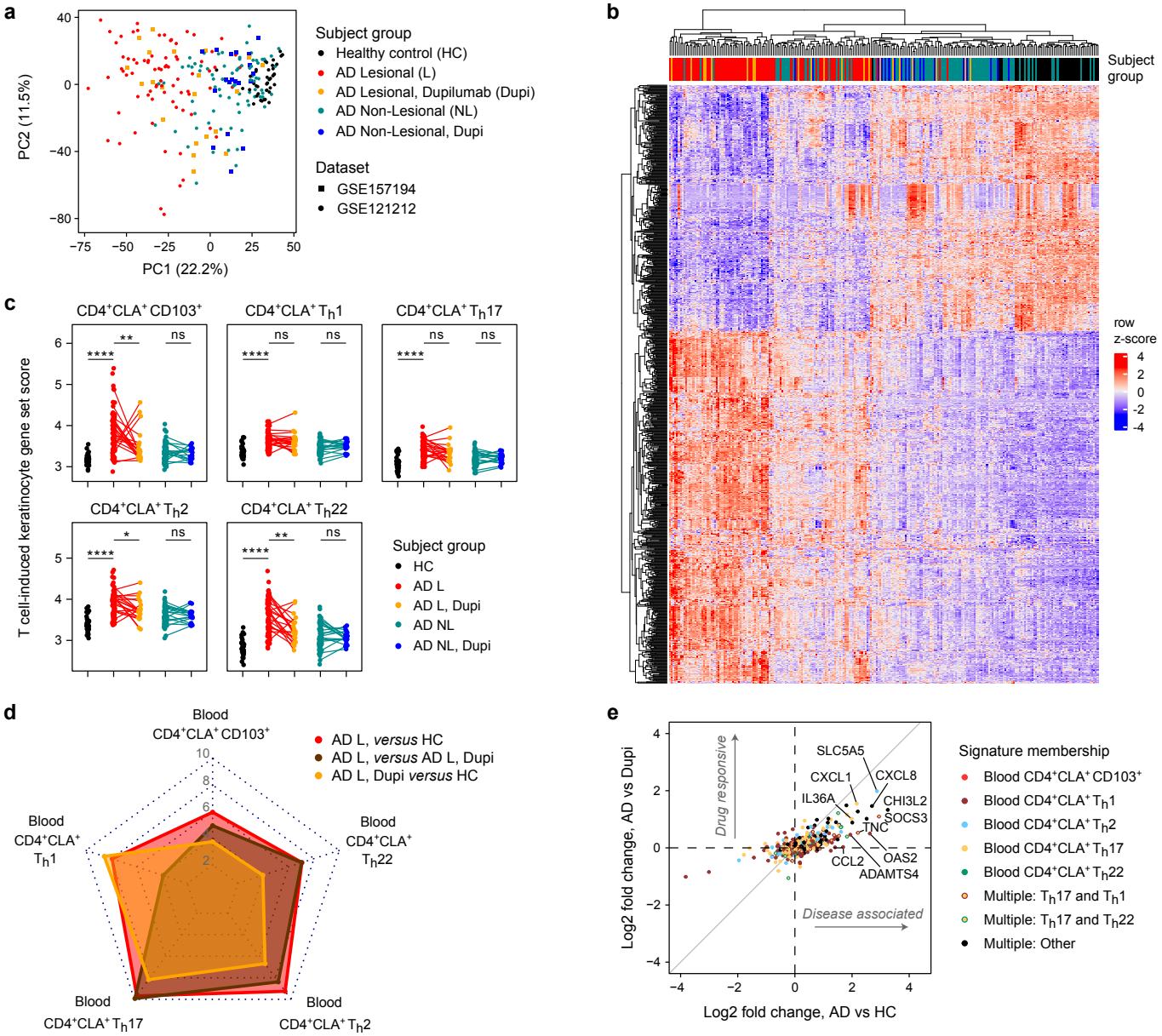

Figure 5. **T cell-dependent gene signatures are enriched in the epidermis during atopic dermatitis and normalized by anti-IL-4Rα therapy**. (**a**) PC analysis of gene expression for AD paired donor lesional and non-lesional skin compared with healthy controls (HC) from the indicated publicly available data sets. AD patients were treated with dupilumab (Dupi), an anti-IL-4Rα drug. Merged data sets were batch corrected to adjust for study-specific effects. (**b**) Heat map showing z-score expression changes of KC genes determined to be T cell-dependent (Figure 2) within public data, as shown in 'a' for the indicated groups. (**c**) Plots showing blood T cell-induced gene set scores, an averaged measure for the effect of each T cell subset on healthy donor KCs per subject group. (**d**) Radar plot showing T cell-induced KC signature gene enrichment values across the indicated pairwise comparisons from public clinical trial data (AD and HC) with -log10 p-values plotted along the radial axis. (**e**) Bivariate plot of the log2 fold change for T cell-dependent KC genes within public clinical trial data from AD or HC subjects (AD vs HC, 'Disease associated'; AD vs anti-IL17A, 'Drug responsive'). Individual genes are colored according to their T cell signature membership. Error bars indicate mean ± SD; ns = not significant, *p ≤ 0.05, **p ≤ 0.01, ***p ≤ 0.001, and ****p ≤ 0.0001 (Student's *t*-test).

Skin CLA$^+$ T cells and the gene signatures they induce in dermal fibroblasts are present in healthy individuals and reduced during inflammatory skin disease

T cell infiltration and aberrant cytokine production cause fibrosis and vascular abnormalities in people with inflammatory disease [56]. SSc is a rare inflammatory condition (~0.1% prevalence in the US) with the highest mortality of any rheumatic illness. In the skin, pathology is associated with elevated T_h2 cell infiltration, myofibroblast and alternatively activated macrophage differentiation [57,58]. Effective therapies for

SSc are severely lacking and ongoing clinical trials are targeting T cell activation and cytokine signaling networks (i.e. IL-4, IL-13, TGFβ, IL-6, JAK/STAT) [59]. Dermal tissue pathology and fibroblast dysfunction has also been described during Ps and is connected to T cell cytokine activity (i.e. IL-17, IL-23, TNFα, IL-36) [60,61]. Despite evidence implicating T cell activity in fibroblast dysregulation, the critical T cell-Fib interactions of healthy and diseased skin have not been established.

To determine whether and to what extent T cell-dependent gene signatures can be found in dermal Fib populations and whether this changes during disease, we analyzed publicly available scRNA-seq data from SSc patients and healthy controls [GSE195452] [3]. In this study, the authors identified 10 transcriptionally distinct Fib subsets including Fib-LGR5, a population that is selectively enriched in healthy skin and significantly diminished with the progression of SSc. The unique functions of these Fib populations and their contribution to disease remain undefined. Our analysis of cells annotated 'fibroblasts' from GSE195452 confirms that the Fib-LGR5 population is preferentially found in healthy skin compared with SSc samples (**Figure 6a, 6b**) and the fraction of Fib-LGR5 is diminished progressively in patients with limited and diffuse disease (**Figure S8a, S8b**). The Fib-MYOC2 and Fib-POSTN subsets were reciprocally elevated in the skin of SSc patients, which correlated with higher autoantibody levels and an increase in skin disease score (**Figure S8b, S8c**). T cell-dependent gene signatures (**Figure 3**) were detected throughout newly described Fib subsets in pooled data from healthy control and SSc subjects. The most pronounced effect observed was the enrichment of skin $CD4^+CLA^+$ T cell-induced genes in the Fib-LGR5 population (**Figure 6c**). The skin $CD4^+CLA^+$ $CD103^+$ T cell-dependent Fib gene signature is specifically elevated in the fraction of Fib-LGR5 cells of healthy donors and reduced in diffuse SSc subject skin while the opposite pattern was seen for the Fib-MYOC2 subset (**Figure 6d**).

We next sought to determine whether transcriptional effects induced by $CD4^+CLA^+$ T cell subsets might contribute to the Ps inflammatory fibroblast axis. Gene expression analysis of skin fibroblasts [GSE173706] [61] showed subject-level distinction between healthy control, non-lesional, and lesional groups (**Figure 6e, S8a**). We observed that both skin $CD4^+CLA^+$ $CD103^{neg}$ and $CD103^+$-induced gene sets (**Figure 3**) are preferentially found in healthy control skin Fibs compared to non-lesional and lesional Ps (**Figure 6f, 6g**). We saw no significant effects when measuring blood $CD4^+CLA^+$-induced Fib genes (**Figure S8d**). We similarly found skin $CD4^+CLA^+$ $CD103^+$ T cell-induced gene programs are reduced in lesional Ps skin compared with paired donor non-lesional biopsies (**Figure 6h-6j, S8a**) in a second Ps clinical cohort [GSE228421] [60]. This study assessed the IL-23 biologic Risankizumab in five Ps subjects, describing dermal fibroblasts gene expression changes occurring over a brief 2-week period after therapy. Consistent with the known role of IL-23 as an activator of the IL-17 signaling cascade, we observed an increase in blood $CD4^+CLA^+$ T_h17-induced signature in fibroblasts from lesional tissue. IL-23 blockade promoted a reversal of the Th17-KC signature back to baseline, but the effect was mixed at the two early timepoints post treatment (**Figure 6j**). We also detected a modest enrichment of blood $CD4^+CLA^+$ $CD103^+$ T cell-induced genes in the lesional Ps group (**Figure S8e**).

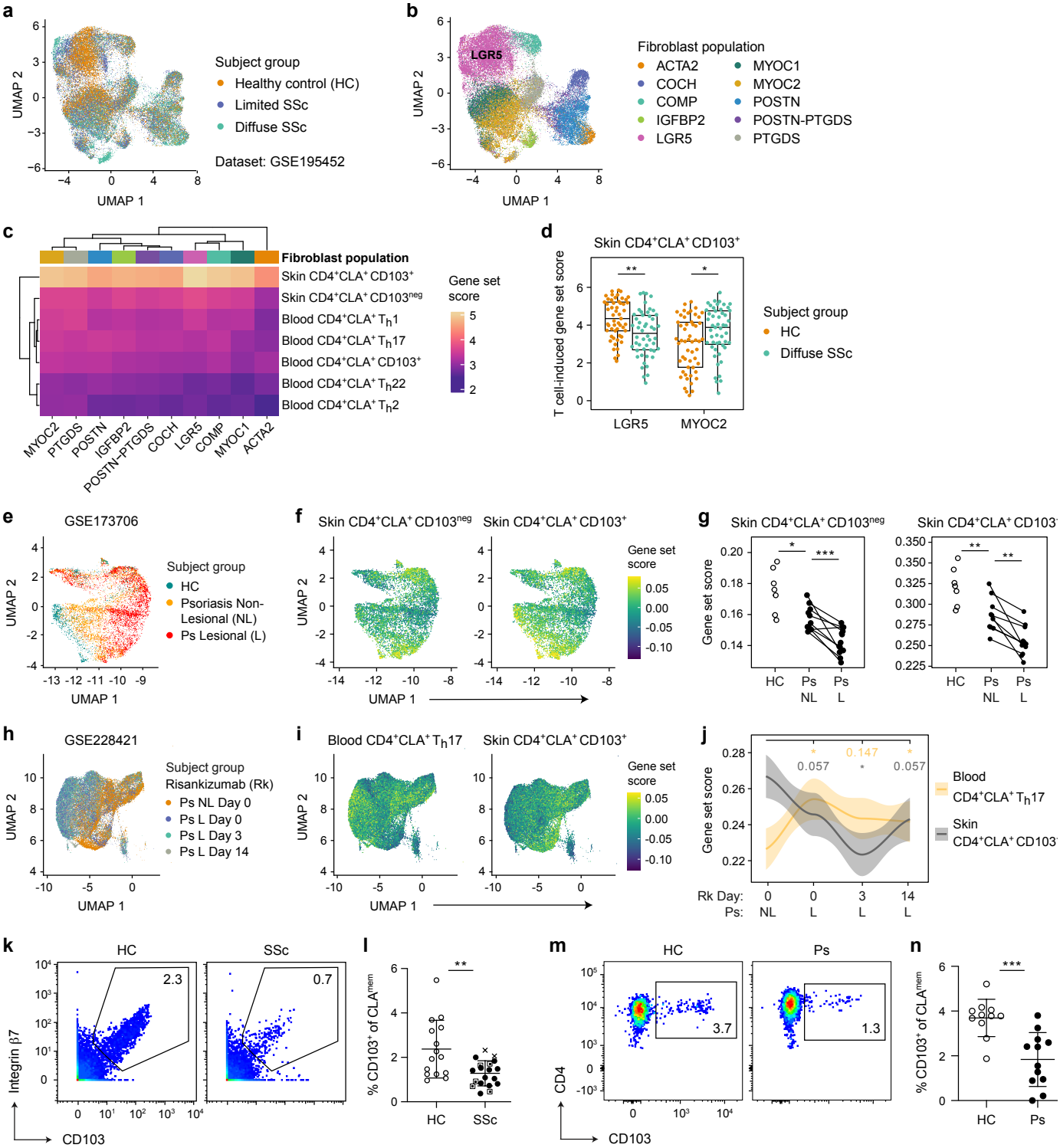

Figure 6. **Skin T cell-induced gene signatures and CD4⁺CLA⁺ CD103⁺ T cells are elevated in healthy subjects and reduced during inflammatory skin disease**. (**a-j**) T cell-induced Fib gene sets (Figure 3) were used to analyze (a-d) public scleroderma and (e-j) psoriasis skin scRNA-seq data, filtered on cells annotated as 'fibroblasts'. Ps lesional and non-lesional skin is from paired donors. (**a-d**) Uniform Manifold Approximation and Projection (UMAP) dimensionality reduction plots showing assignment by (a) subject group and (b) defined Fib subset [GSE195452]. (c) Heat map showing the enrichment of T cell-dependent gene signatures for each Fib population pooled across all subject groups. (d) Plot showing T cell-dependent gene signature enrichment in Fib subsets, pseudobulked at the subject level. (**e-g**) UMAP plots showing assignment (e) by subject group and (f) skin T cell-dependent gene set enrichment, (g) quantified per group [GSE173706]. (h-j) UMAP plots of patient data [GSE228421] before (Day 0) and after (Days 3, 14) IL-23 blockade (Risankizumab, Rk) showing assignment (h) by subject group and (i) T cell-dependent gene set enrichment, (j) quantified per group. (**k-m**) Cytometric analysis of blood CD4⁺CLA⁺ CD103⁺ T cells. (k) Representative fluorescence cytometry plots and (l) quantification of T cells in HC (n=15) or SSc (n=19) patient blood, gated on CD103, integrin β7, and pre-gated on CLA^{mem}, as in Figure 1. SSc samples: circle = limited disease, square = diffuse, X = unclassified. (m) Representative mass cytometry plots and (n) quantification of T cells in HC (n=11) or Ps (n=12) patient blood, gated on CLA^{mem}, as in Figure S8. Error bars indicate mean ± SD; ns = not significant, *p ≤ 0.05, **p ≤ 0.01, ***p ≤ 0.001, and ****p ≤ 0.0001 (d, Student's *t*-test; l,n, Mann-Whitney U).

301 $CD4^+CLA^+$ $CD103^+$ T cells in the blood represent a migratory fraction of T_{RM} that express a
302 transcriptional and cytokine profile indicative of a role in wound healing and tissue repair [11]. As $CD4^+CLA^+$
303 $CD103^+$ T cell-induced gene signatures are altered between healthy control and diseased subject skin, we
304 sought to determine if T cell abundance was also impacted. We measured the frequency of $CD4^+CLA^+$
305 $CD103^+$ T cells in the blood of SSc and Ps patients and found a reduction in both disease groups with
306 respect to matched healthy controls (**Figure 6k-6n, S8f**), suggesting that the regulation of the $CD103^+$ T cell
307 population is important during inflammatory skin disease. Thus, we show that skin $CD4^+CLA^+$ T cell activity
308 supports the transcriptional programs of healthy skin-associated Fibs and that $CD103^+$ T cells in circulation
309 are diminished during inflammatory skin disease.
310

311 **DISCUSSION**

312 In this study, we constructed an atlas of T cell-induced gene states in human skin – a catalog of epidermal
313 keratinocyte and dermal fibroblast transcriptional reprogramming by different $CD4^+CLA^+$ T_h cell populations
314 – then applied our findings towards a deeper understanding of clinical data sets. Although the use of CLA to
315 track cutaneous T cells goes back nearly three decades, [8,9] our approach uniquely combines CLA
316 identification of both blood- and skin-derived T_h cells together with chemokine receptor gating strategies and
317 CD103 designation of migratory T_{RM} [10,11] to isolate broad and functionally diverse $CD4^+CLA^+$ T_h cells, which
318 we leverage to study the changing transcriptional landscape of healthy and inflamed human skin.
319 T cells elicited significant effects on both primary KCs and Fibs, substantially altering the transcriptional
320 landscape of each cell type. Cytokine-dependent gene modules were broadly enriched, especially through
321 the activity of blood-derived CLA^+ T cells. This included expected gene set enrichment such as CLA^+ T_h1-
322 mediated IFN-associated gene expression, and CLA^+ T_h2-mediated IL-4 and IL-13 responses in both KCs
323 and Fibs. Skin-derived T cells were instead more likely to promote gene networks required to execute
324 critical homeostatic functions of skin. Keratinization, cornification, and proliferation processes – essential for
325 maintenance and renewal of a healthy epithelium [62] – were induced specifically in KCs by $CD103^{neg}$ or
326 $CD103^+$ skin T cells, while metal ion response pathways involved in wound healing [23] were induced by
327 $CD103^{neg}$ T cells, which was only observed in Fibs. Our findings demonstrate the broad functional capacity
328 of each these T cell populations and suggest how changes in the $CD4^+CLA^+$ pool would impact both the
329 inflammatory response against harmful pathogens and the upkeep of homeostatic tissue functions such as
330 barrier maintenance, recovery from injury, and regulated self-renewal.
331 Blocking T cell cytokine responses during Ps (i.e. IL-17) and AD (i.e. IL-4/IL-13) reduces leukocyte
332 accumulation in the tissue and reverses skin pathology. While many studies have shown the efficacy of
333 these drugs, not all patients meet the desired clinical endpoints and severe adverse events occur in a small
334 but significant proportion of individuals, warranting further investigation to define the mechanisms of drug
335 action and to identify new candidate drugs as alternative therapies [63–68]. TNFα or IL-23 blocking therapies,
336 for example, offer substitutes for Ps patients failing anti-IL-17A therapy, and the IL-13 specific agonist

337 tralokinumab is an alternative to dupilumab in AD. Establishing biomarkers of disease and the response to
338 therapy will help guide the most effective course of treatment on an individual patient level. Our study adds
339 important context that can help interpret clinical outcomes following anti-cytokine therapy. We describe the
340 T cell-dependent gene networks in KCs that are enriched in lesional skin of Ps and AD patients compared
341 with non-lesional and healthy controls, and we demonstrate how the expression of specific T-dependent
342 genes are impacted during anti-cytokine therapy in patient skin.

343 By combining this approach with public immunogenetics data from Ps patients, we identified CCL20,
344 CCL8, and IL19 as T_h17 cell-induced targets of anti-IL-17A therapy. Expression of each of these genes is
345 elevated in lesional skin compared with controls, returned to baseline following therapy, and each contains
346 GWAS risk alleles for Ps that are eQTL. Taken together with published studies, our findings suggest these
347 genes are part of a cooperative functional network that promotes Ps: CCL20 recruits IL-17 producing
348 disease-associated $CCR6^+$ T_h17 cells to the skin; [48,69] CCL8 recruits $CCR5^+$ $CD4^+$ T cells that are involved
349 in barrier integrity maintenance and implicated in Ps pathogenesis; [70,71] IL-19 expression is positively
350 associated with Psoriasis Area and Severity Index – a measure of skin pathology. Expression of IL-19 is
351 both IL-17-dependent and further enhances the effects of IL-17A, increasing IL-23p19 expression and
352 production of CCL20 [49]. IL-19 is part of the IL-23/IL-17 inflammatory signaling network of Ps and is a
353 proposed biomarker of disease. Guselkumab (anti-IL-23) is an approved drug for Ps that showed superior
354 long-term efficacy to secukinumab, [72] but no current therapy targets other components of the T cell/KC/Ps
355 axis we describe such as IL-19, CCL8, or skin-tropic $CCR5^+$ T cells.

356 We also describe genes that are uniquely induced by CLA^+ T_h2 cells in KCs, which are significantly
357 altered in lesional AD patient skin and responsive to dupilumab. For example, CA2 was previously shown to
358 be induced in KCs and engineered skin equivalents by IL-4 and IL-13 [55,73]. In comparison NTRK1, an early
359 IL-13 target involved in allergic responses, is not clearly connected to AD [74], and our findings suggest a
360 stronger link. Other genes we identify, such as TNC, CHI3L2 and SLC5A5, were shown to be upregulated in
361 AD patient lesional skin, [75–77] but further research is required to determine the relevance of these factors in
362 disease and the response to treatment. Importantly, some *but not all* T-dependent KC genes enriched in
363 lesional patient skin are responsive to biologic therapy, which could indicate the presence of stable
364 epigenetic changes imprinted during disease. Our study establishes a strategy to assess the transcriptional
365 response to biologics, which could help identify novel cellular and genetic targets for future therapeutic
366 intervention.

367 Our analyses of skin Fib responses suggests that a balance of functionally distinct CLA^+ T cell
368 populations is critical to Ps and SSc disease progression. We show across multiple patient cohorts and
369 diseases that skin $CD4^+CLA^+$ $CD103^+$ T cells support the gene programs of healthy dermal populations such
370 as Fib-LGR5 that are significantly reduced during SSc. This raises the possibility that $CD4^+CLA^+$ $CD103^+$ T
371 cell activity is directly required to maintain Fib-LGR5 and that loss or dysregulation of these T cells
372 contributes to the development of myofibroblasts known to drive fibrosis such as Fib-MYOC2, -SFRP2, or -

373 PRSS23 [5,78]. The LGR5 expressing population is transcriptionally similar to Fib-PI16 described previously, [2]
374 with both Fib-LGR5 and -PI16 independently shown to be reduced in SSc patient skin [3,79]. Individuals with
375 severe SSc and reduced Fib-LGR5 are the most likely to have anti-topoisomerase I (scl-70) autoantibodies,
376 which puts them at the highest risk for severe pulmonary fibrosis and end-organ disease [80], reinforcing the
377 importance of understanding immune-based regulation of healthy skin-associated Fibs.

378 Previously, we published that skin $CD4^+CLA^+$ $CD103^+$ T_{RM} cells uniquely co-produce IL-13 and IL-22 and
379 have a TGFβ gene signature, implicating them in tissue repair, barrier maintenance, and homeostatic
380 function [11]. We now report that the migratory fraction of $CD4^+CLA^+$ $CD103^+$ T cells in the blood is reduced in
381 both SSc and Ps patients, supporting the notion that these cells are important to disease development.
382 Whether these T cells are also altered in the skin, if they become dysfunctional during disease, and if they
383 directly impact the activity or survival of disease-relevant populations in the skin such as Fib-LGR5 remain
384 open, yet exciting questions. A therapeutic strategy focused on reinforcing the function or number or healthy
385 skin-associated T cell and Fib populations could be a useful adjunct to anti-cytokine therapies that are
386 aimed at minimizing the impact of deleterious immune cells.

387 Our study design and subsequent analysis contain some caveats and limitations. First, we measure 13
388 analytes produced by activated T cells, which accounts for only a fraction of the cytokines, metabolites and
389 other soluble factors that are part of the T cell-dependent regulation of skin structural cell gene programs.
390 Second, our study uses KCs and Fibs from a single anatomical skin site and donor. Thus, we are unable to
391 comment on site-specific differences, for example owing to changes in moisture content, microbiome, or
392 hair follicle density across this large barrier tissue, or population level variability in T cell-induced responses.
393 Finally, the data from several publicly available interventional clinical trials that we assessed in this study
394 were generated using either bulk sequencing or microarray methods, and some were smaller studies with
395 limited power. Additionally, not all data sets we assessed showed a significant enrichment of T cell-
396 dependent gene programs (*data not shown*) [2,5,79,81]. Future analyses are required to validate the essential T
397 cell- and cytokine-directed gene networks in KC or Fib subsets during health and disease across this large
398 barrier tissue.

399 The atlas of T cell-dependent gene expression responses that we introduce in this study represents a
400 new tool to facilitate a deeper understanding of the complex biology and transcriptional networks of skin.
401 Using our data to deconvolute published clinical studies has yielded new insights into immune-directed
402 pathogenesis of Ps, AD, and SSc, and demonstrates the importance of T cells in the upkeep of structural
403 cell subsets in healthy skin. Thus, our study presents and validates a broadly applicable, systems-based
404 approach to dissecting the immune-dependent contributions to tissue homeostasis, inflammation, and
405 fibrosis.

406 **MATERIALS AND METHODS**

407 **Human subject enrollment and study design**

408 The objective of this research was to characterize the effect of human T cells on the gene expression profile
409 of epithelial KCs and dermal Fibs. Immune cell isolation was performed using healthy blood and skin tissue
410 – donor range 32 to 71 years of age. Human skin was obtained from patients undergoing elective surgery –
411 panniculectomy or abdominoplasty. The cohort size was selected to ensure a greater than 80% probability
412 of identifying an effect of >20% in measured variables. All samples (**Table S5**) were obtained upon written
413 informed consent at Virginia Mason Franciscan Health (Seattle, WA, USA) and the Dr. D. Y. Patil Medical
414 College, Hospital, and Research Centre (Pune, India). All study protocols were conducted according to
415 Declaration of Helsinki principles and approved by the Institutional Review Board of Benaroya Research
416 Institute (Seattle, WA, USA), the Institutional Human Ethics Committees of Dr. D. Y. Patil Medical College,
417 Hospital, and Research Centre (Pune, India) and CSIR – Institute of Genomics and Integrative Biology
418 (New Delhi, India).

419

420 **Sex as a biological variable**

421 Our study examined both male and female tissue with similar findings reported for both sexes. The study
422 was not powered to detect sex-based differences.

423

424 **Isolation of T cells from blood**

425 PBMC were isolated using Ficoll-Hypaque (GE-Healthcare; GE17-1440-02) gradient separation. T cells
426 were enriched using CD4 microbeads (Miltenyi; 130-045-101) then rested overnight at a concentration of 2
427 x 10^6 cells/mL in ImmunoCult™-XF T Cell Expansion Medium (StemCell; 10981) with 1%
428 penicillin/streptomycin (Sigma-Aldrich; P0781) in a 15 cm^2 dish. The next morning cells were harvested and
429 prepared for cell sorting, as indicated.

430

431 **Isolation of T cells from skin**

432 Fresh surgical discards of abdominal skin were treated with PBS + 0.1% Primocin (Invitrogen; ant-pm-1) for
433 5 minutes to eliminate contaminating microorganisms. Sterile tissue processing was performed on ice and
434 skin was periodically sprayed with 1x PBS to keep samples from drying out. A biopsy tool (Integra™
435 Miltex™) was used to excise 4mm tissue biopsies from each sample. The subcutaneous fat was removed
436 from biopsies before an overnight digestion of approximately 16 hours at 37°C, 5%CO_2. The digestion mix
437 contained 0.8 mg/mL Collagenase Type 4 (Worthington; LS004186) and 0.04 mg/mL DNase (Sigma-
438 Aldrich; DN25) in RPMI supplemented with 10% pooled male human serum (Sigma-Aldrich; H4522, lot
439 SLC0690), 2 mM L-glutamine, 100 U/mL penicillin, and 100 mg/mL streptomycin. We used 1 mL of RPMI
440 digestion media for each 40-50mg tissue in a 6-well non-tissue culture treated dish. The next morning tissue
441 samples were washed excess RPMI + 3% FBS and combined into a single tube per donor. Filtration on a

442 100μM membrane was performed at each wash step, five total on average, to generate a single-cell
443 suspension of skin mononuclear cells free of contaminating fat and debris. Skin mononuclear cell
444 suspensions were then prepared for cell sorting, as indicated.
445
446 **Cytometry and cell sorting**
447 *Fluorescence cytometry* – Cell labelling of surface antigens on blood- and skin-derived T cells was
448 performed using fluorescently tagged antibodies diluted in cell staining buffer containing HBSS and 0.3%
449 BSA (**Table S6**). Viability dye staining using Fixable LiveDead was performed first in HBSS containing no
450 additional protein, as recommended by the manufacturer. Surface staining was performed at 5% CO_2, 37°C
451 for 20 minutes. Labeled cells were then either acquired on a BD LSR™ Fortessa cell analyzer or prepared
452 for cell sorting.
453 *Cell sorting* – Fluorescently labelled samples were placed in cell sorting buffer – for yield sorts, HBSS +
454 5.0% BSA, for purity sorts HBSS + 1.0% BSA – using a BD FACSAria™ Fusion (85μM nozzle, 45 p.s.i.).
455 The indicated conventional T_h cell populations (T_{Conv}) were sorted from blood and T_{Reg} were excluded by
456 purity sort following $CD4^+$ T cell microbead enrichment. Skin mononuclear preparations were first enriched
457 by a CD3 yield sort followed by purity sort of $CD4^+$ T_{Conv} and exclusion of T_{Reg}. Additional sample collection
458 was performed using the BD LSR™ Fortessa cell analyzer.
459 *Mass cytometry* – Frozen PBMC samples were prepared as described, then rested overnight in
460 ImmunoCult™-XF T Cell Expansion Medium supplemented with 1% penicillin/streptomycin and 5% human
461 serum. Human pan T cell isolation was performed (Miltenyi; 130-096-535) and 0.5 x 10^6 to 2 x 10^6 purified T
462 cells were stained for analysis, as follows. Cell viability staining using 5 μM Cisplatin (Enzo Life Sciences;
463 ALX-400-040) in PBS. After 1 minute at room temperature the reaction was quenched. Metal-tagged
464 antigen labeling using antibody cocktail (**Table S6**) diluted in Maxpar® Cell Staining Buffer (Standard
465 BioTools; 201068) for 30 minutes at room temperature. Labeled cells were resuspended with Maxpar
466 Intercalator-Ir intact stain in Fix and Perm Buffer at 4°C, overnight (Fluidigm; 201192A and 201067). Cells
467 were resuspended in ultrapure water containing 1/5th volume EQ Four Element Calibration Beads (Standard
468 BioTools; 201078) and acquired on a Standard BioTools CyTOF Helios at an event rate of 300-400 cells per
469 second. Samples were processed in four subsequent batches over the course of one week. All
470 fluorescence and mass cytometry data (.FCS 3.0 or .FCS 3.1) were analyzed using FlowJo software (BD,
471 v.10.9).
472
473 **T cell stimulation and cytometric quantification of cytokines**
474 Sorted T cell populations were pelleted by centrifugation at 300 x g for 5 minutes and resuspend in
475 ImmunoCult™-XF T Cell Expansion Medium with 1% penicillin/streptomycin. Cultured T cells were
476 stimulated for 48 hours at 1 x 10^6 cells/mL with ImmunoCult™ Human αCD3/αCD28/αCD2 T Cell Activator
477 reagent (StemCell; 10970) used at the manufacturer recommended concentration. Cytokine containing

478 supernatants from each unique donor were harvested and stored at -20C°. Frozen blood and skin activated
479 T cell supernatants from all donors were thawed as a single batch to assess cytokine concentrations by
480 cytometric bead array (BioLegend; LEGENDplex™ reagent) using a custom analyte panel: GM-CSF, IFNγ,
481 IL-2, IL-4, IL-5, IL-6, IL-9, IL-10, IL-13, IL-17A, IL-17F, IL-22, TNFα. Data were analyzed using the
482 manufacturer provided LEGENDplex software. The remaining thawed T cell supernatants were used
483 immediately, without additional freeze-thaws, in culture of KCs or Fibs, as described. Unstimulated controls
484 were generated using a single freeze-thawed aliquot of cell-free ImmunoCult™-XF T Cell Expansion
485 Medium.
486
487 **Keratinocyte and fibroblast cell culture and activation**
488 Paired primary human epithelial KCs and dermal Fibs from the eyelid of a single healthy donor were
489 purchased from a commercial vendor (ZenBio; KR-F or DF-F) and cultured at low passages (p = 2-7) using
490 either the KGM™ Keratinocyte Growth Medium BulletKit™ (Lonza; CC-3111) for KCs or DMEM
491 supplemented with 10% FBS, 2 mM L-glutamine, 100 U/ml penicillin, and 100 mg/ml streptomycin (Gibco™;
492 10938025) for Fibs. Cytokine containing T cell supernatants were diluted using a 1:1 ratio of appropriate cell
493 culture media and added to KCs or Fibs growing at 50% confluence – approximately 1-2 x 10^4 – in a 96-well
494 flat bottom plate. Structural cells were cultured with activated T cell supernatants for 24 hours prior to
495 isolation for RNA-sequencing (RNA-seq). Unstimulated controls received a 1:1 ratio of fresh T cell media
496 combined with either KC or Fib culture media.
497
498 **Bulk RNA-sequencing (RNA-seq)**
499 High-quality total RNA was isolated from approximately 2 x 10^4 T cell supernatant-treated KCs or Fibs using
500 TRIzol™ Reagent (Invitrogen™; 15596026). Next, cDNA was prepared using the SMART-Seq v4 Ultra Low
501 Input RNA Kit for Sequencing (Takara). Library construction was performed using the NexteraXT DNA
502 sample preparation kit (Illumina) using half the recommended volumes and reagents. Dual-index, single-
503 read sequencing of pooled libraries was run on a HiSeq2500 sequencer (Illumina) with 58-base reads and a
504 target depth of 5 million reads per sample. Base-calling and demultiplexing were performed automatically
505 on BaseSpace (Illumina) to generate FASTQ files.
506
507 **Analysis of bulk RNA-seq data**
508 The FASTQ files were processed to remove reads of zero length (fastq_trimmer v.1.0.0), remove adapter
509 sequences (fastqmcf tool v.1.1.2), and perform quality trimming from both ends until a minimum base
510 quality ≥ 30 (FASTQ quality trimmer tool v.1.0.0). Reads were aligned to the human reference genome
511 (build hg38) with TopHat (v.1.4.0) and read counts per Ensembl gene ID were quantified with htseq-count
512 (v.0.4.1). Quality metrics for the FASTQ and BAM/SAM files were generated with FastQC (v.0.11.3) and
513 Picard (v.1.128). Processing of FASTQ and BAM/SAM files was executed on the Galaxy workflow platform

514 of Globus genomics. Statistical analysis of gene expression was assessed in the R environment (v.4.3.2).
515 Sample inclusion for final analysis was based on a set of pre-established quality control criteria: total
516 number of fastq reads > 1 x 10^6; mapped reads > 70%; median CV coverage < 0.85. Randomization was
517 not applicable as no treatment or intervention groups were included in the study. Blinding was not
518 applicable as no treatment groups were compared.
519
520 **Additional bioinformatic analyses**
521 All differential expression and pathway enrichment analyses were performed in R. To assess differential
522 expression, the limma package (v.3.58.1) was used [82]. A log2 expression fold change of at least 1 in
523 magnitude and an FDR of less than 0.05 were used as cutoffs to define differentially expressed genes.
524 Individual blood- and skin-T cell subset induced gene sets were formed by first filtering out any differentially
525 expressed genes shared across all treatment groups – broadly excluding non-specific T cell effects on
526 keratinocytes or fibroblasts – and then selecting up to the top 200 differentially upregulated genes ranked by
527 FDR and associated with a T cell subset stimulation condition.
528 In analysis of public bulk microarray and RNA-seq GEO datasets, the ComBat function from the sva
529 package (v.3.50.0) was used to adjust for dataset-specific batch effects [83]. Pathway enrichment analysis
530 was performed using the enrichR package (v.3.2) [84] with the Reactome 2022 database [85] to query pathways
531 associated with T cell-induced genes. T cell signatures were treated as a custom database and expression
532 of these signatures were examined as lists of differentially expressed genes associated with Ps or AD.
533 GWAS hits associated with the trait "psoriasis" were downloaded from the NHGRI-EBI GWAS Catalog
534 on February 7th, 2024. Within these results, GWAS SNPs with a "DISEASE/TRAIT" value of "Generalized
535 pustular psoriasis", "COVID-19 or psoriasis (trans-disease meta-analysis)", or "Paradoxical eczema in
536 biologic-treated plaque psoriasis" were excluded to ensure Ps-specific SNPs were analyzed [86].
537 Single cell gene expression data from SSc and Ps cohort studies was re-analyzed using the Seurat R
538 package (v.4) [87]. CellTypist was used to identify fibroblasts using an adult human skin reference model [88–90].
539 For SSc public data, pseudobulking was applied to defined SSc Fib clusters [GSE195452] [3]. The average
540 expression of T cell-induced genes was then computed for each pseudobulk profile as a gene set score. For
541 Ps public data, pseudobulking was applied to tissue type or subject/visit group as indicated [GSE173706] [61]
542 and [GSE228421] [60]. The average expression of T cell-induced genes was then computed for each
543 pseudobulk profile as a gene set score. Gene set scores for individual cells were computed using the
544 AddModuleScores() method within Seurat [91].
545
546 **DATA AVAILABILITY STATEMENT**
547 Values for all data points presented in figure graphs are reported in the **Supporting Data Values** file. All
548 gene expression data sets generated in this study are available to the public in the Gene Expression
549 Omnibus, **GSE272623**. Computer code generated and used for analysis in this study is available in Github:

Commit URL, https://github.com/BenaroyaResearch/Morawski-T-cell-transcriptional-programs-in-skin; Commit ID, ab964c4.

ORCiDs

Hannah A. DeBerg: https://orcid.org/0000-0002-5263-158X
Mitch L. Fahning: https://orcid.org/0000-0001-9352-4409
Suraj R. Varkhande: https://orcid.org/0000-0001-8813-0907
James D. Schlenker: https://orcid.org/0009-0000-8223-0333
William P. Schmitt: https://orcid.org/0009-0009-1202-9111
Aayush Gupta: https://orcid.org/0000-0002-1455-8086
Archana Singh: https://orcid.org/0000-0003-1388-9489
Iris K. Gratz: https://orcid.org/0000-0001-7470-7277
Jeffrey S. Carlin: https://orcid.org/0009-0006-5634-1981
Daniel J. Campbell: https://orcid.org/0000-0002-9652-7178
Peter A. Morawski: https://orcid.org/0000-0001-9159-4032

CONFLICT OF INTEREST STATEMENT

The authors declare no competing interests.

ACKNOWLEDGEMENTS

We are grateful to: Kassidy Benoscek-Narag, Sylvia Posso, Thien-Son Nguyen, and the Clinical Research Center coordinators in the Benaroya Research Institute (BRI) Center for Interventional Immunology for human subject recruitment, sample collection and screening; the BRI Genomics, Flow Cytometry, and Human Immunophenotyping facilities for technical assistance and expertise; the BRI Scientific Writing Group for critical reading of the text. BRI cytometry and genomics equipment used in this study were generously supported by the M.J. Murdock Charitable Trust. This work was supported by a New Investigator research award (National Scleroderma Foundation) and R21AI185642 (NIAID, NIH) to PAM, R01AI127726 to IKG and DJC (NIAID, NIH), and R01AI169893 to HAD, IKG and DJC (NIAID, NIH).

AUTHOR CONTRIBUTIONS (CrediT STATEMENT)

Conceptualization: HAD, IKG, JSC, DJC, PAM; Data Curation: HAD; Formal Analysis: HAD, DJC, PAM; Funding Acquisition: HAD, IKG, DJC, PAM; Investigation: HAD, MLF, SRV, AS, PAM; Methodology: HAD, DJC, PAM; Project administration: PAM; Software: HAD; Resources: JDS, WPS, AG, AS, JSC; Supervision: IKG, DJC, PAM; Validation: HAD, PAM; Visualization: HAD, DJC, PAM; Writing – original draft: HAD, PAM; Writing – review and editing: HAD, IKG, DJC, PAM.

586 **SUPPLEMENTARY MATERIAL**

587 **Figures S1-S8**. Supplementary figures.

588 **Document S1**. Supporting data values for all Figures.

589 **Table S1**. Comprehensive statistics for Figures 1 and S1.

590 **Table S2**. Comprehensive statistics for Figure S3.

591 **Table S3**. Comprehensive statistics for Figure S5.

592 **Table S4**. Comprehensive statistics for Figure S6.

593 **Table S5**. Patient cohort information.

594 **Table S6**. Flow and mass cytometry antibody information.

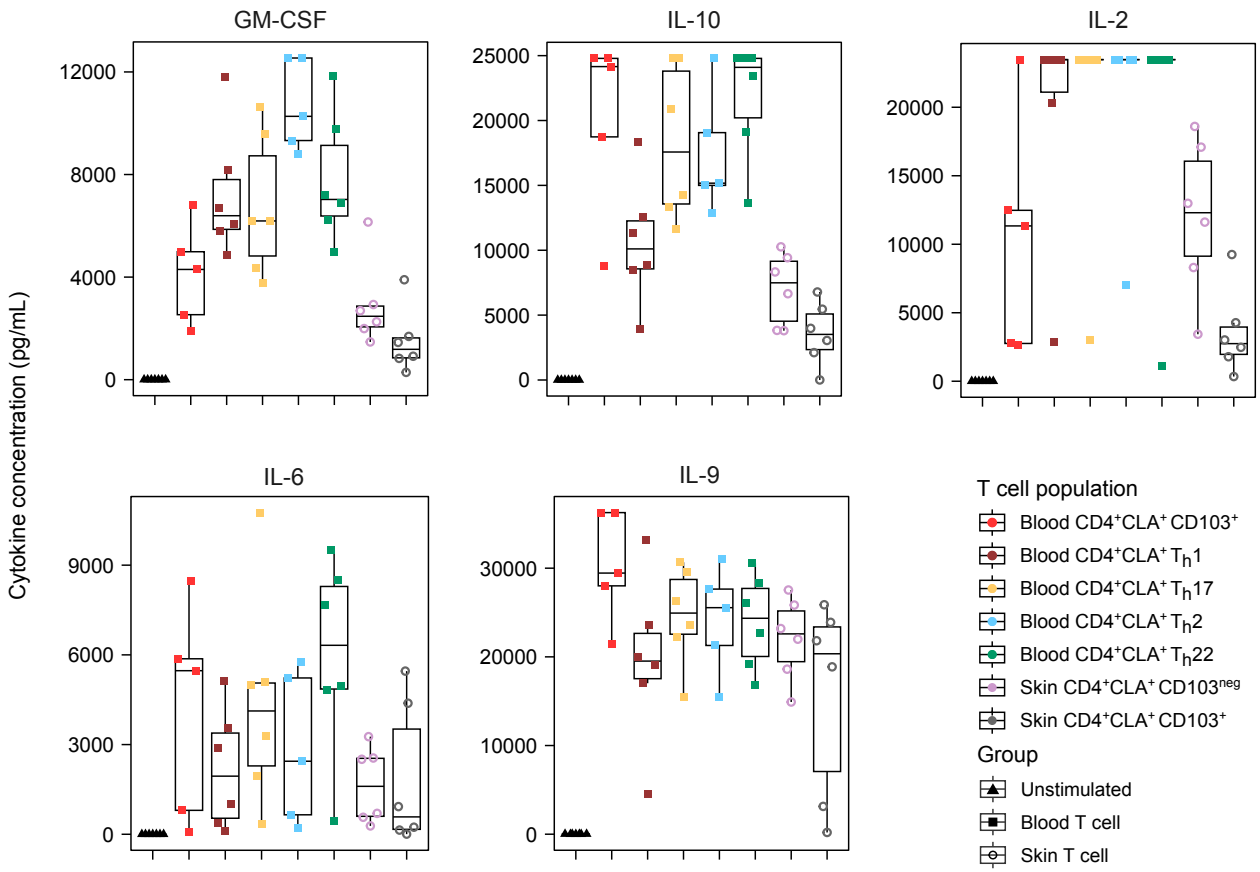

Figure S1 (related to Figure 1). **Additional cytokine production capacity by circulating and skin-resident human CD4$^+$CLA$^+$ T cell populations**. Quantitative cytokine bead array measurement of all stimulated T cell supernatants for the 5 indicated analytes (n=5-6 donors per population). Full statistical analysis of cytokine production is provided in **Table S1**.

595

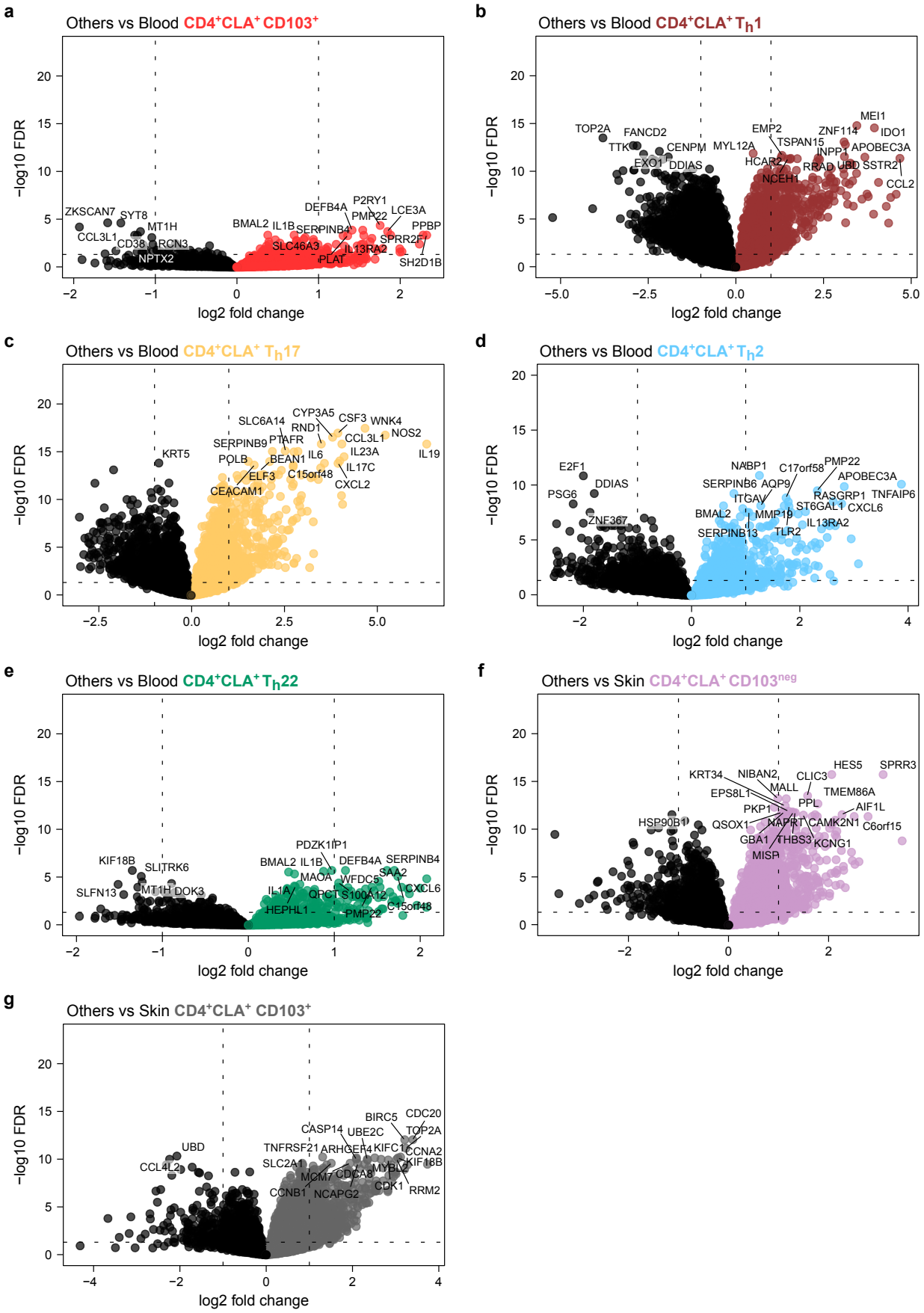

Figure S2 (related to Figure 2). **CD4⁺CLA⁺ T cell-induced differential gene expression analysis of epithelial keratinocytes**. (**a-g**) Volcano plots showing differential gene expression analysis for KCs stimulated with each indicated CD4⁺CLA⁺ T_h population. Cutoffs: log2 fold change >1 and -log10 FDR <0.05. The top 20 genes, ranked by FDR, are labeled on each plot.

596

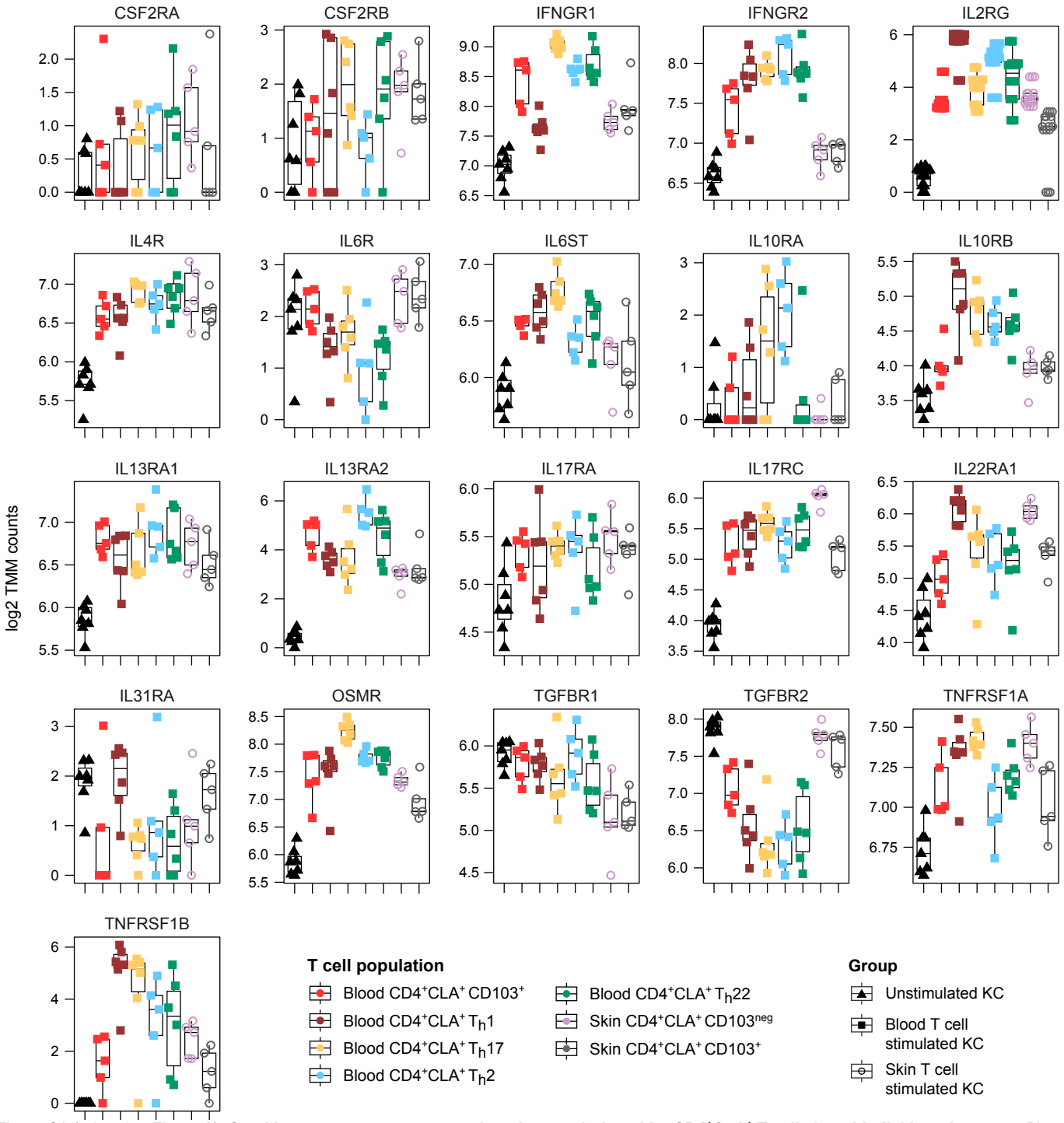

Figure S3 (related to Figure 2). **Cytokine receptor gene expression changes induced by CD4⁺CLA⁺ T cells in epithelial keratinocytes**. Plots of log2 normalized expression counts using trimmed mean of M values (TMM) for each cytokine receptor gene in KCs stimulated with the indicated T cell populations (n=5-6 donors per population). Full statistical analysis of cytokine receptor gene expression is provided in **Table S2**.

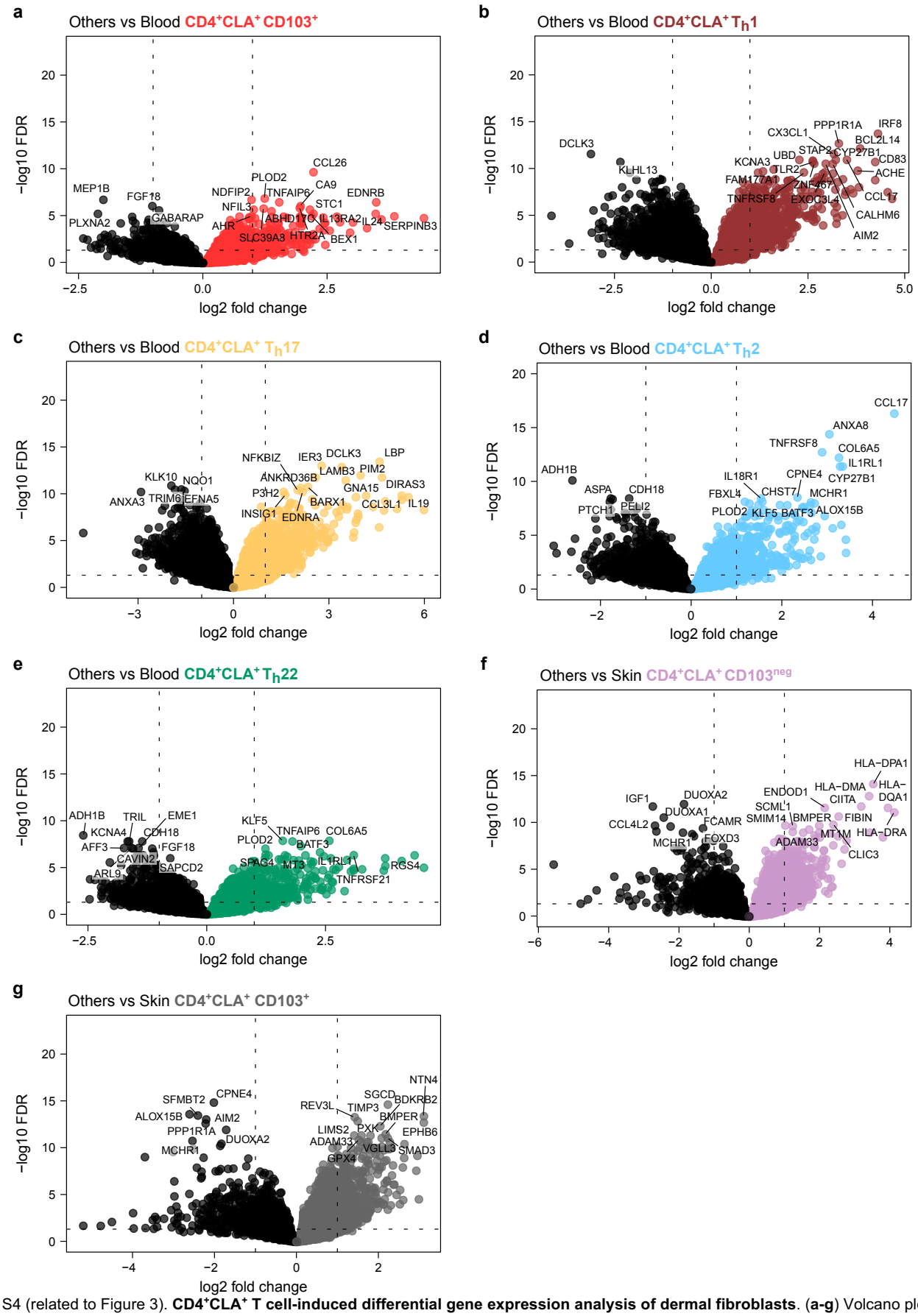

Figure S4 (related to Figure 3). **CD4⁺CLA⁺ T cell-induced differential gene expression analysis of dermal fibroblasts**. (**a-g**) Volcano plots showing differential gene expression analysis for Fibs stimulated with each indicated CD4⁺CLA⁺ T_h population. Cutoffs: log2 fold change >1 and -log10 FDR <0.05. The top 20 genes, ranked by FDR, are labeled on each plot.

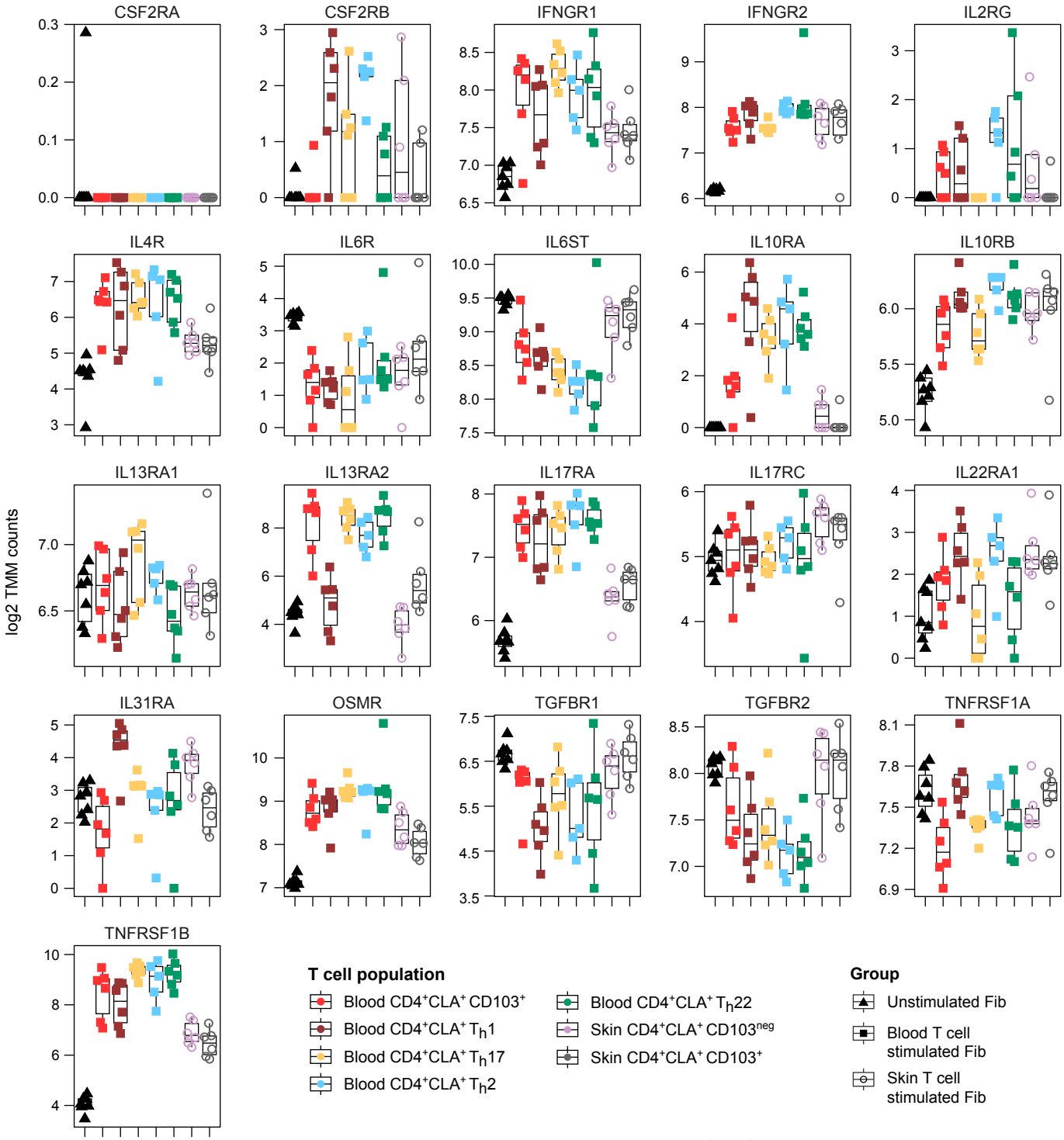

Figure S5 (related to Figure 3). **Cytokine receptor gene expression changes induced by CD4$^+$CLA$^+$ T cells in dermal fibroblasts**. Plots of log2 normalized expression counts using trimmed mean of M values (TMM) for each cytokine receptor gene in Fibs stimulated with the indicated T cell populations (n=5-6 donors per population). Full statistical analysis of cytokine receptor gene expression is provided in **Table S3**.

a

	GSE137218	GSE166388	GSE31652
Samples (#)	84	8	30
Donors (#)	14	8	17
Disease group	Psoriasis	Psoriasis, Healthy Control	Psoriasis
Treatment	Secukinumab	None	Ixekizumab, Placebo
Tissue type	Lesional, Non-Lesional	Lesional, Healthy	Lesional
Visit (Days)	0, 4, 14, 42, 84	n/a	0, 14

b

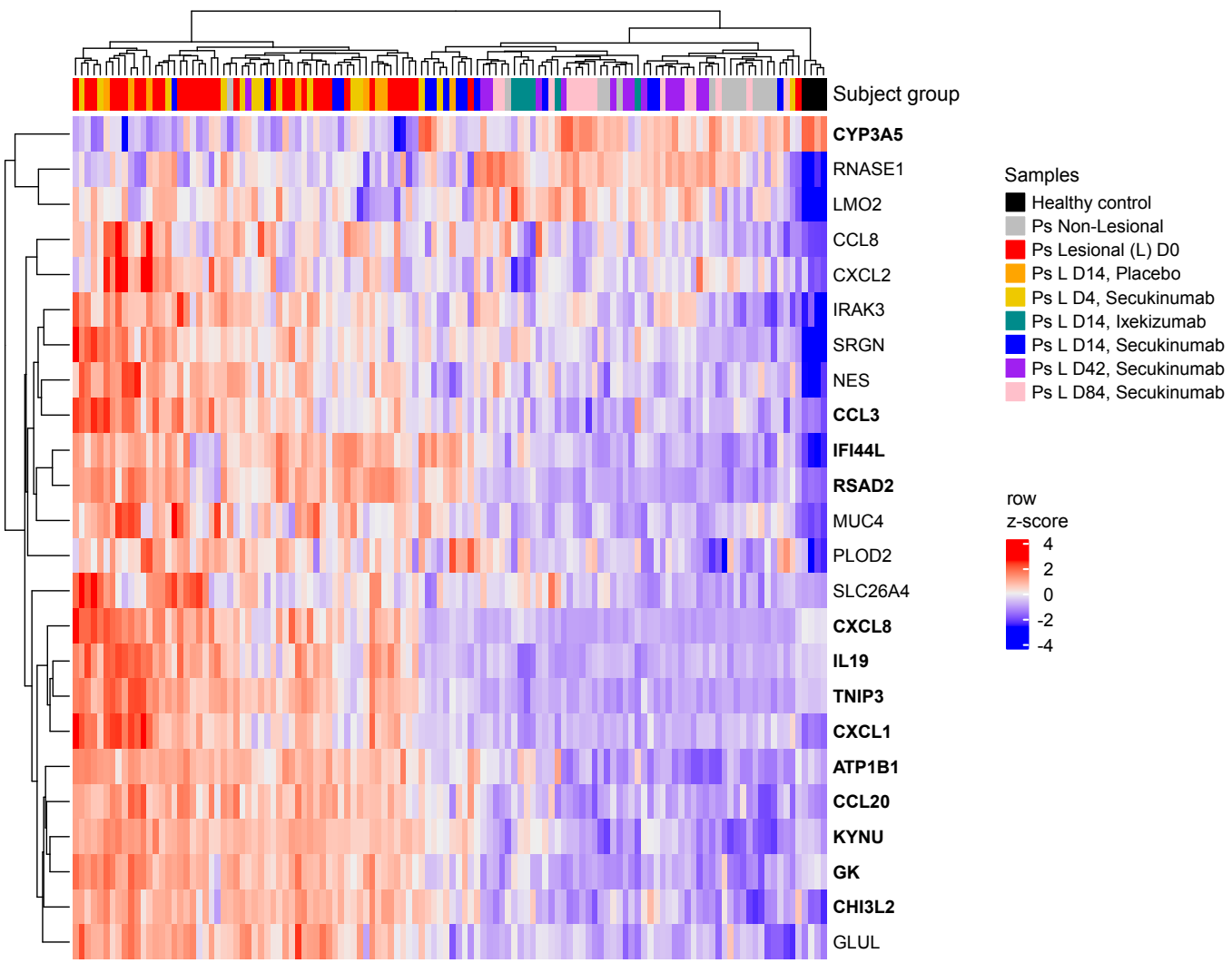

Figure S6 (related to Figure 4). **CD4$^+$CLA$^+$ T$_h$17-dependent genes are altered in psoriasis patients undergoing anti-IL-17A therapy**. (**a**) Summary table showing cohort information for each of the three public Ps clinical trial data sets analyzed in Figure 4. (**b**) Heat map showing z-score expression changes of KC genes determined to be T$_h$17-dependent (Figure 2) within publicly available Ps patient data shown in Figure 4 for the indicated groups. Bolded genes are those that are significantly impacted by anti-IL-17A therapy compared with Ps Lesional D0. Full statistical analysis of T$_h$17-dependent gene expression is provided in **Table S4**.

a

	GSE157194	GSE121212
Samples (#)	151	94
Donors (#)	57	44
Disease group	Atopic Dermatitis	Atopic Dermatitis, Healthy Control
Treatment	Dupilumab	None
Tissue type	Lesional, Non-Lesional	Healthy, Lesional, Non-Lesional
Visit (Months)	0, 3	n/a

b

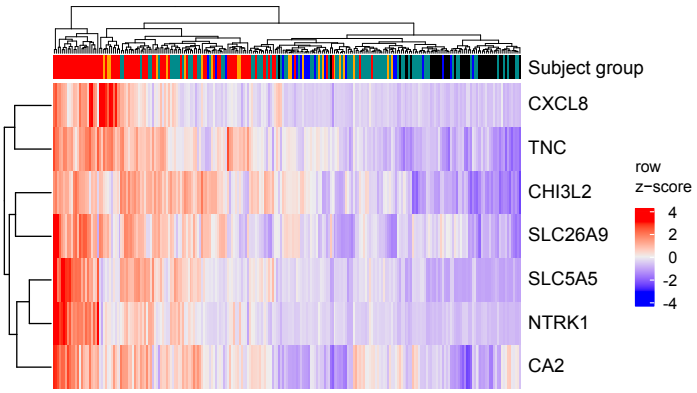

c

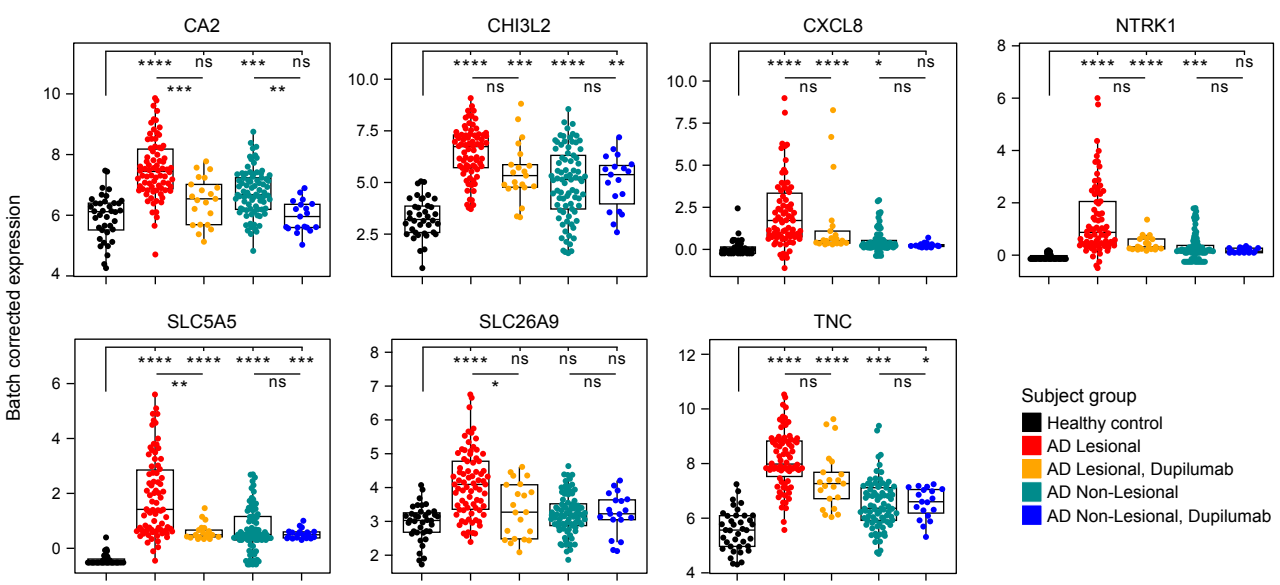

Figure S7 (related to Figure 5). **CD4⁺CLA⁺ T_h2-dependent genes are altered in atopic dermatitis patients undergoing anti-IL-4Rα therapy**. (**a**) Summary table showing cohort information for the two public AD clinical trial data sets analyzed in Figure 5. (**b**) Heat map showing z-score expression changes of KC genes determined to be T_h2-dependent (Figure 2) within publicly available AD patient clinical data shown in Figure 5 for the indicated groups. (**c**) Individual gene plots for each T_h2-dependent KC gene identified within public AD clinical trial data sets. Error bars indicate mean ± SD; ns = not significant, *p ≤ 0.05, **p ≤ 0.01, ***p ≤ 0.001, and ****p ≤ 0.0001 (Student's *t*-test).

601

a

	GSE195452	GSE173706	GSE228421
Samples (#)	153	33	20
Donors (#)	153	21	5
Subject group	Systemic sclerosis (SSc), Healthy Control (HC)	Psoriasis (Ps), HC	Ps, HC
Treatment	None	None	Risankizumab (Rk)
Tissue type	Affected-Diffuse, Affected-Limited, Healthy	Non-Lesional (NL), Lesional (L), Healthy	NL, Healthy
Visit (Days)	n/a	n/a	0, 3, 14

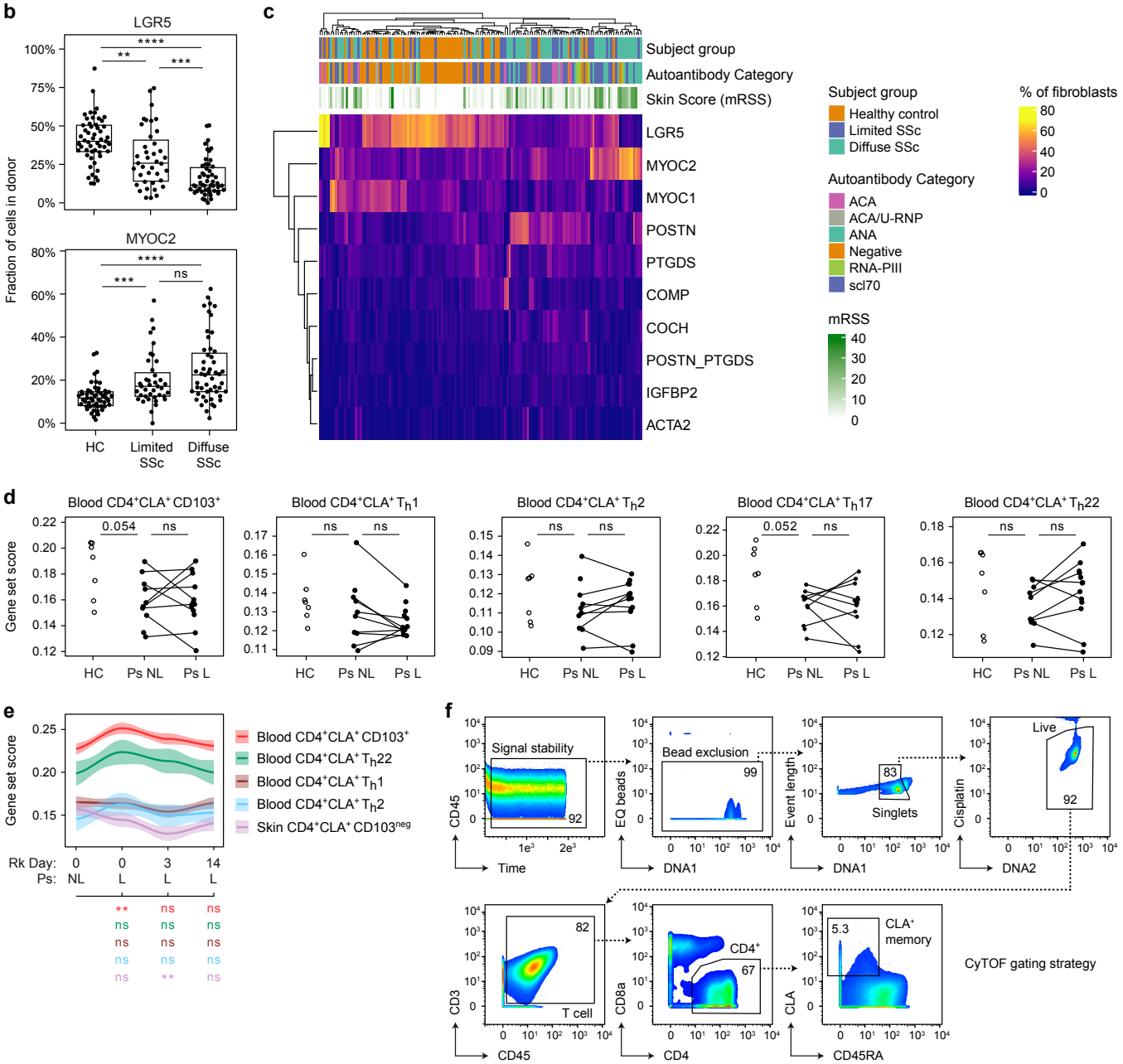

Figure S8 (related to Figure 6). **Dermal fibroblast subsets and T cell-dependent fibroblast gene programs are altered between healthy control and inflammatory skin disease subjects**. (**a**) Summary table showing cohort information for public data sets analyzed in Figure 6. (**b,c**) Analysis of public scleroderma skin scRNA-seq data [GSE195452]. (b) Plots show the frequency of disease-altered Fib subsets for each subject group. Single cell data are pseudobulked at the subject level. (c) Heat map shows indicated Fib subsets as a percentage of total dermal fibroblasts (*rows*) for each donor (*columns*) including Group, Autoantibody Category, and Skin Score (mRSS). ACA, anti-centromere antibody; U-RNP, U1 small nuclear ribonucleoprotein particle; ANA, anti-nuclear antibody; Neg, auto-antibody negative; RNA-PIII, RNA polymerase III; scl70, scleroderma 70kDa/DNA-topoisomerase-1; mRSS, modified Rodnan skin score. (**d**) Quantification of T cell-dependent Fib gene set enrichment per subject group for public single cell Ps skin data [GSE173706]. (**e**) Indicated T cell-dependent gene set enrichment in single cell skin data of each subject group [GSE228421] undergoing treatment (Tx) with Risankizumab (α-IL-23). (**f**) Mass cytometry identification strategy for CLA^{memory} T cells in donor blood. Error bars indicate mean ± SD; ns = not significant, *p ≤ 0.05, **p ≤ 0.01, ***p ≤ 0.001, and ****p ≤ 0.0001 (Student's *t*-test).

603 **REFERENCES**

604 1. Cheng, J.B., Sedgewick, A.J., Finnegan, A.I., Harirchian, P., Lee, J., Kwon, S., Fassett, M.S., Golovato, J.,
605 Gray, M., Ghadially, R., et al. (2018). Transcriptional Programming of Normal and Inflamed Human
606 Epidermis at Single-Cell Resolution. Cell Rep *25*, 871–883. https://doi.org/10.1016/j.celrep.2018.09.006.

607 2. Buechler, M.B., Pradhan, R.N., Krishnamurty, A.T., Cox, C., Calviello, A.K., Wang, A.W., Yang, Y.A., Tam,
608 L., Caothien, R., Roose-Girma, M., et al. (2021). Cross-tissue organization of the fibroblast lineage. Nature
609 *593*, 575–579. https://doi.org/10.1038/s41586-021-03549-5.

610 3. Gur, C., Wang, S.-Y., Sheban, F., Zada, M., Li, B., Kharouf, F., Peleg, H., Aamar, S., Yalin, A.,
611 Kirschenbaum, D., et al. (2022). LGR5 expressing skin fibroblasts define a major cellular hub perturbed in
612 scleroderma. Cell *185*, 1373-1388.e20. https://doi.org/10.1016/j.cell.2022.03.011.

613 4. Tabib, T., Morse, C., Wang, T., Chen, W., and Lafyatis, R. (2018). SFRP2/DPP4 and FMO1/LSP1 Define
614 Major Fibroblast Populations in Human Skin. J Invest Dermatol *138*, 802–810.
615 https://doi.org/10.1016/j.jid.2017.09.045.

616 5. Tabib, T., Huang, M., Morse, N., Papazoglou, A., Behera, R., Jia, M., Bulik, M., Monier, D.E., Benos, P.V.,
617 Chen, W., et al. (2021). Myofibroblast transcriptome indicates SFRP2hi fibroblast progenitors in systemic
618 sclerosis skin. Nat Commun *12*, 4384. https://doi.org/10.1038/s41467-021-24607-6.

619 6. Ho, A.W., and Kupper, T.S. (2019). T cells and the skin: from protective immunity to inflammatory skin
620 disorders. Nat Rev Immunol *19*, 490–502. https://doi.org/10.1038/s41577-019-0162-3.

621 7. Sender, R., Weiss, Y., Navon, Y., Milo, I., Azulay, N., Keren, L., Fuchs, S., Ben-Zvi, D., Noor, E., and Milo,
622 R. (2023). The total mass, number, and distribution of immune cells in the human body. Proc Natl Acad Sci
623 U S A *120*, e2308511120. https://doi.org/10.1073/pnas.2308511120.

624 8. Fuhlbrigge, R.C., Kieffer, J.D., Armerding, D., and Kupper, T.S. (1997). Cutaneous lymphocyte antigen is a
625 specialized form of PSGL-1 expressed on skin-homing T cells. Nature *389*, 978–981.
626 https://doi.org/10.1038/40166.

627 9. Clark, R.A., Chong, B., Mirchandani, N., Brinster, N.K., Yamanaka, K.-I., Dowgiert, R.K., and Kupper, T.S.
628 (2006). The vast majority of CLA+ T cells are resident in normal skin. J Immunol *176*, 4431–4439.
629 https://doi.org/10.4049/jimmunol.176.7.4431.

630 10. Duhen, T., Duhen, R., Lanzavecchia, A., Sallusto, F., and Campbell, D.J. (2012). Functionally distinct
631 subsets of human FOXP3+ Treg cells that phenotypically mirror effector Th cells. Blood *119*, 4430–4440.
632 https://doi.org/10.1182/blood-2011-11-392324.

633 11. Klicznik, M.M., Morawski, P.A., Höllbacher, B., Varkhande, S.R., Motley, S.J., Kuri-Cervantes, L.,
634 Goodwin, E., Rosenblum, M.D., Long, S.A., Brachtl, G., et al. (2019). Human CD4+CD103+ cutaneous
635 resident memory T cells are found in the circulation of healthy individuals. Sci Immunol *4*, eaav8995.
636 https://doi.org/10.1126/sciimmunol.aav8995.

637 12. Kortekaas Krohn, I., Aerts, J.L., Breckpot, K., Goyvaerts, C., Knol, E., Van Wijk, F., and Gutermuth, J.
638 (2022). T-cell subsets in the skin and their role in inflammatory skin disorders. Allergy *77*, 827–842.
639 https://doi.org/10.1111/all.15104.

640 13. Sabat, R., Wolk, K., Loyal, L., Döcke, W.-D., and Ghoreschi, K. (2019). T cell pathology in skin
641 inflammation. Semin Immunopathol *41*, 359–377. https://doi.org/10.1007/s00281-019-00742-7.

642 14. Duffin, K.C., and Krueger, G.G. (2009). Genetic variations in cytokines and cytokine receptors associated
643 with psoriasis found by genome-wide association. J Invest Dermatol *129*, 827–833.
644 https://doi.org/10.1038/jid.2008.308.

645 15. Stadler, R., Mayer-da-Silva, A., Bratzke, B., Garbe, C., and Orfanos, C. (1989). Interferons in
646 dermatology. J Am Acad Dermatol *20*, 650–656. https://doi.org/10.1016/s0190-9622(89)70078-5.

647 16. Chan, T.C., Hawkes, J.E., and Krueger, J.G. (2018). Interleukin 23 in the skin: role in psoriasis
648 pathogenesis and selective interleukin 23 blockade as treatment. Ther Adv Chronic Dis *9*, 111–119.
649 https://doi.org/10.1177/2040622318759282.

650 17. Silfvast-Kaiser, A., Paek, S.Y., and Menter, A. (2019). Anti-IL17 therapies for psoriasis. Expert Opin Biol
651 Ther *19*, 45–54. https://doi.org/10.1080/14712598.2019.1555235.

652 18. Song, A., Lee, S.E., and Kim, J.H. (2022). Immunopathology and Immunotherapy of Inflammatory Skin
653 Diseases. Immune Netw *22*, e7. https://doi.org/10.4110/in.2022.22.e7.

654 19. Deckers, J., Anbergen, T., Hokke, A.M., de Dreu, A., Schrijver, D.P., de Bruin, K., Toner, Y.C., Beldman,
655 T.J., Spangler, J.B., de Greef, T.F.A., et al. (2023). Engineering cytokine therapeutics. Nat Rev Bioeng *1*, 286–
656 303. https://doi.org/10.1038/s44222-023-00030-y.

657 20. Höllbacher, B., Duhen, T., Motley, S., Klicznik, M.M., Gratz, I.K., and Campbell, D.J. (2020).
658 Transcriptomic Profiling of Human Effector and Regulatory T Cell Subsets Identifies Predictive Population
659 Signatures. Immunohorizons *4*, 585–596. https://doi.org/10.4049/immunohorizons.2000037.

660 21. de Jesús-Gil, C., Sans-de SanNicolàs, L., García-Jiménez, I., Ferran, M., Celada, A., Chiriac, A., Pujol, R.M.,
661 and Santamaria-Babí, L.F. (2021). The Translational Relevance of Human Circulating Memory Cutaneous
662 Lymphocyte-Associated Antigen Positive T Cells in Inflammatory Skin Disorders. Front Immunol *12*, 652613.
663 https://doi.org/10.3389/fimmu.2021.652613.

664 22. Kominsky, D.J., Campbell, E.L., Ehrentraut, S.F., Wilson, K.E., Kelly, C.J., Glover, L.E., Collins, C.B.,
665 Bayless, A.J., Saeedi, B., Dobrinskikh, E., et al. (2014). IFN-γ-mediated induction of an apical IL-10 receptor
666 on polarized intestinal epithelia. J Immunol *192*, 1267–1276. https://doi.org/10.4049/jimmunol.1301757.

667 23. Jenkins, W., Perone, P., Walker, K., Bhagavathula, N., Aslam, M.N., DaSilva, M., Dame, M.K., and Varani,
668 J. (2011). Fibroblast response to lanthanoid metal ion stimulation: potential contribution to fibrotic tissue
669 injury. Biol Trace Elem Res *144*, 621–635. https://doi.org/10.1007/s12011-011-9041-x.

670 24. Fichtner-Feigl, S., Strober, W., Kawakami, K., Puri, R.K., and Kitani, A. (2006). IL-13 signaling through the
671 IL-13alpha2 receptor is involved in induction of TGF-beta1 production and fibrosis. Nat Med *12*, 99–106.
672 https://doi.org/10.1038/nm1332.

673 25. Chao, H., Zheng, L., Hsu, P., He, J., Wu, R., Xu, S., Zeng, R., Zhou, Y., Ma, H., Liu, H., et al. (2023). IL-
674 13RA2 downregulation in fibroblasts promotes keloid fibrosis via JAK/STAT6 activation. JCI Insight *8*,
675 e157091. https://doi.org/10.1172/jci.insight.157091.

676 26. Dillon, S.R., Sprecher, C., Hammond, A., Bilsborough, J., Rosenfeld-Franklin, M., Presnell, S.R., Haugen,
677 H.S., Maurer, M., Harder, B., Johnston, J., et al. (2004). Interleukin 31, a cytokine produced by activated T
678 cells, induces dermatitis in mice. Nat Immunol *5*, 752–760. https://doi.org/10.1038/ni1084.

679 27. Bilsborough, J., Leung, D.Y.M., Maurer, M., Howell, M., Boguniewicz, M., Yao, L., Storey, H., LeCiel, C.,
680 Harder, B., and Gross, J.A. (2006). IL-31 is associated with cutaneous lymphocyte antigen-positive skin
681 homing T cells in patients with atopic dermatitis. J Allergy Clin Immunol *117*, 418–425.
682 https://doi.org/10.1016/j.jaci.2005.10.046.

683 28. Vu, T.T., Koguchi-Yoshioka, H., and Watanabe, R. (2021). Skin-Resident Memory T Cells: Pathogenesis
684 and Implication for the Treatment of Psoriasis. J Clin Med *10*, 3822. https://doi.org/10.3390/jcm10173822.

685 29. Esaki, H., Brunner, P.M., Renert-Yuval, Y., Czarnowicki, T., Huynh, T., Tran, G., Lyon, S., Rodriguez, G.,
686 Immaneni, S., Johnson, D.B., et al. (2016). Early-onset pediatric atopic dermatitis is TH2 but also TH17
687 polarized in skin. J Allergy Clin Immunol *138*, 1639–1651. https://doi.org/10.1016/j.jaci.2016.07.013.

688 30. Tsoi, L.C., Rodriguez, E., Degenhardt, F., Baurecht, H., Wehkamp, U., Volks, N., Szymczak, S., Swindell,
689 W.R., Sarkar, M.K., Raja, K., et al. (2019). Atopic Dermatitis Is an IL-13-Dominant Disease with Greater
690 Molecular Heterogeneity Compared to Psoriasis. J Invest Dermatol *139*, 1480–1489.
691 https://doi.org/10.1016/j.jid.2018.12.018.

692 31. Gittler, J.K., Shemer, A., Suárez-Fariñas, M., Fuentes-Duculan, J., Gulewicz, K.J., Wang, C.Q.F., Mitsui, H.,
693 Cardinale, I., de Guzman Strong, C., Krueger, J.G., et al. (2012). Progressive activation of T(H)2/T(H)22
694 cytokines and selective epidermal proteins characterizes acute and chronic atopic dermatitis. J Allergy Clin
695 Immunol *130*, 1344–1354. https://doi.org/10.1016/j.jaci.2012.07.012.

696 32. Aboobacker, S., Kurn, H., and Al Aboud, A.M. (2024). Secukinumab. In StatPearls (StatPearls Publishing).

697 33. Preuss, C.V., and Quick, J. (2024). Ixekizumab. In StatPearls (StatPearls Publishing).

698 34. Gade, A., Ghani, H., Patel, P., and Rubenstein, R. (2024). Dupilumab. In StatPearls (StatPearls
699 Publishing).

700 35. Guttman-Yassky, E., Kabashima, K., Staumont-Salle, D., Nahm, W.K., Pauser, S., Da Rosa, J.C., Martel,
701 B.C., Madsen, D.E., Røpke, M., Arlert, P., et al. (2024). Targeting IL-13 with tralokinumab normalizes type 2
702 inflammation in atopic dermatitis both early and at 2 years. Allergy *79*, 1560–1572.
703 https://doi.org/10.1111/all.16108.

704 36. Ganier, C., Mazin, P., Herrera-Oropeza, G., Du-Harpur, X., Blakeley, M., Gabriel, J., Predeus, A.V., Cakir,
705 B., Prete, M., Harun, N., et al. (2024). Multiscale spatial mapping of cell populations across anatomical sites
706 in healthy human skin and basal cell carcinoma. Proc Natl Acad Sci U S A *121*, e2313326120.
707 https://doi.org/10.1073/pnas.2313326120.

708 37. Herrera-Acosta, E., Garriga-Martina, G.G., Suárez-Pérez, J.A., Martínez-García, E.A., and Herrera-
709 Ceballos, E. (2020). Comparative study of the efficacy and safety of secukinumab vs ixekizumab in
710 moderate-to-severe psoriasis after 1 year of treatment: Real-world practice. Dermatol Ther *33*, e13313.
711 https://doi.org/10.1111/dth.13313.

38. Bertelsen, T., Ljungberg, C., Litman, T., Huppertz, C., Hennze, R., Rønholt, K., Iversen, L., and Johansen, C. (2020). IκBζ is a key player in the antipsoriatic effects of secukinumab. J Allergy Clin Immunol *145*, 379–390. https://doi.org/10.1016/j.jaci.2019.09.029.

39. Qiu, X., Zheng, L., Liu, X., Hong, D., He, M., Tang, Z., Tian, C., Tan, G., Hwang, S., Shi, Z., et al. (2021). ULK1 Inhibition as a Targeted Therapeutic Strategy for Psoriasis by Regulating Keratinocytes and Their Crosstalk With Neutrophils. Front Immunol *12*, 714274. https://doi.org/10.3389/fimmu.2021.714274.

40. Krueger, J.G., Fretzin, S., Suárez-Fariñas, M., Haslett, P.A., Phipps, K.M., Cameron, G.S., McColm, J., Katcherian, A., Cueto, I., White, T., et al. (2012). IL-17A is essential for cell activation and inflammatory gene circuits in subjects with psoriasis. J Allergy Clin Immunol *130*, 145-154.e9. https://doi.org/10.1016/j.jaci.2012.04.024.

41. Ellinghaus, D., Jostins, L., Spain, S.L., Cortes, A., Bethune, J., Han, B., Park, Y.R., Raychaudhuri, S., Pouget, J.G., Hübenthal, M., et al. (2016). Analysis of five chronic inflammatory diseases identifies 27 new associations and highlights disease-specific patterns at shared loci. Nat Genet *48*, 510–518. https://doi.org/10.1038/ng.3528.

42. Folkersen, L., Gustafsson, S., Wang, Q., Hansen, D.H., Hedman, Å.K., Schork, A., Page, K., Zhernakova, D.V., Wu, Y., Peters, J., et al. (2020). Genomic and drug target evaluation of 90 cardiovascular proteins in 30,931 individuals. Nat Metab *2*, 1135–1148. https://doi.org/10.1038/s42255-020-00287-2.

43. Dimas, A.S., Deutsch, S., Stranger, B.E., Montgomery, S.B., Borel, C., Attar-Cohen, H., Ingle, C., Beazley, C., Gutierrez Arcelus, M., Sekowska, M., et al. (2009). Common regulatory variation impacts gene expression in a cell type-dependent manner. Science *325*, 1246–1250. https://doi.org/10.1126/science.1174148.

44. Quach, H., Rotival, M., Pothlichet, J., Loh, Y.-H.E., Dannemann, M., Zidane, N., Laval, G., Patin, E., Harmant, C., Lopez, M., et al. (2016). Genetic Adaptation and Neandertal Admixture Shaped the Immune System of Human Populations. Cell *167*, 643-656.e17. https://doi.org/10.1016/j.cell.2016.09.024.

45. Liu, J.Z., van Sommeren, S., Huang, H., Ng, S.C., Alberts, R., Takahashi, A., Ripke, S., Lee, J.C., Jostins, L., Shah, T., et al. (2015). Association analyses identify 38 susceptibility loci for inflammatory bowel disease and highlight shared genetic risk across populations. Nat Genet *47*, 979–986. https://doi.org/10.1038/ng.3359.

46. Li, Y.R., Li, J., Zhao, S.D., Bradfield, J.P., Mentch, F.D., Maggadottir, S.M., Hou, C., Abrams, D.J., Chang, D., Gao, F., et al. (2015). Meta-analysis of shared genetic architecture across ten pediatric autoimmune diseases. Nat Med *21*, 1018–1027. https://doi.org/10.1038/nm.3933.

47. Javierre, B.M., Burren, O.S., Wilder, S.P., Kreuzhuber, R., Hill, S.M., Sewitz, S., Cairns, J., Wingett, S.W., Várnai, C., Thiecke, M.J., et al. (2016). Lineage-Specific Genome Architecture Links Enhancers and Non-coding Disease Variants to Target Gene Promoters. Cell *167*, 1369-1384.e19. https://doi.org/10.1016/j.cell.2016.09.037.

48. Furue, K., Ito, T., Tsuji, G., Nakahara, T., and Furue, M. (2020). The CCL20 and CCR6 axis in psoriasis. Scand J Immunol *91*, e12846. https://doi.org/10.1111/sji.12846.

749 49. Witte, E., Kokolakis, G., Witte, K., Philipp, S., Doecke, W.-D., Babel, N., Wittig, B.M., Warszawska, K.,
750 Kurek, A., Erdmann-Keding, M., et al. (2014). IL-19 is a component of the pathogenetic IL-23/IL-17 cascade
751 in psoriasis. J Invest Dermatol *134*, 2757–2767. https://doi.org/10.1038/jid.2014.308.

752 50. Furue, M., Furue, K., Tsuji, G., and Nakahara, T. (2020). Interleukin-17A and Keratinocytes in Psoriasis.
753 Int J Mol Sci *21*, 1275. https://doi.org/10.3390/ijms21041275.

754 51. Watarai, A., Amoh, Y., Maejima, H., Hamada, Y., and Katsuoka, K. (2013). Nestin expression is increased
755 in the suprabasal epidermal layer in psoriasis vulgaris. Acta Derm Venereol *93*, 39–43.
756 https://doi.org/10.2340/00015555-1420.

757 52. Möbus, L., Rodriguez, E., Harder, I., Stölzl, D., Boraczynski, N., Gerdes, S., Kleinheinz, A., Abraham, S.,
758 Heratizadeh, A., Handrick, C., et al. (2021). Atopic dermatitis displays stable and dynamic skin
759 transcriptome signatures. J Allergy Clin Immunol *147*, 213–223. https://doi.org/10.1016/j.jaci.2020.06.012.

760 53. Tsoi, L.C., Rodriguez, E., Stölzl, D., Wehkamp, U., Sun, J., Gerdes, S., Sarkar, M.K., Hübenthal, M., Zeng,
761 C., Uppala, R., et al. (2020). Progression of acute-to-chronic atopic dermatitis is associated with quantitative
762 rather than qualitative changes in cytokine responses. J Allergy Clin Immunol *145*, 1406–1415.
763 https://doi.org/10.1016/j.jaci.2019.11.047.

764 54. Kamsteeg, M., Jansen, P. a. M., van Vlijmen-Willems, I.M.J.J., van Erp, P.E.J., Rodijk-Olthuis, D., van der
765 Valk, P.G., Feuth, T., Zeeuwen, P.L.J.M., and Schalkwijk, J. (2010). Molecular diagnostics of psoriasis, atopic
766 dermatitis, allergic contact dermatitis and irritant contact dermatitis. Br J Dermatol *162*, 568–578.
767 https://doi.org/10.1111/j.1365-2133.2009.09547.x.

768 55. Kamsteeg, M., Bergers, M., de Boer, R., Zeeuwen, P.L.J.M., Hato, S.V., Schalkwijk, J., and Tjabringa, G.S.
769 (2011). Type 2 helper T-cell cytokines induce morphologic and molecular characteristics of atopic dermatitis
770 in human skin equivalent. Am J Pathol *178*, 2091–2099. https://doi.org/10.1016/j.ajpath.2011.01.037.

771 56. Wynn, T.A., and Ramalingam, T.R. (2012). Mechanisms of fibrosis: therapeutic translation for fibrotic
772 disease. Nat Med *18*, 1028–1040. https://doi.org/10.1038/nm.2807.

773 57. Fang, D., Chen, B., Lescoat, A., Khanna, D., and Mu, R. (2022). Immune cell dysregulation as a mediator
774 of fibrosis in systemic sclerosis. Nat Rev Rheumatol *18*, 683–693. https://doi.org/10.1038/s41584-022-
775 00864-7.

776 58. Gabrielli, A., Avvedimento, E.V., and Krieg, T. (2009). Scleroderma. N Engl J Med *360*, 1989–2003.
777 https://doi.org/10.1056/NEJMra0806188.

778 59. Mulcaire-Jones, E., Low, A.H.L., Domsic, R., Whitfield, M.L., and Khanna, D. (2023). Advances in
779 biological and targeted therapies for systemic sclerosis. Expert Opinion on Biological Therapy *23*, 325–339.
780 https://doi.org/10.1080/14712598.2023.2196009.

781 60. Francis, L., McCluskey, D., Ganier, C., Jiang, T., Du-Harpur, X., Gabriel, J., Dhami, P., Kamra, Y.,
782 Visvanathan, S., Barker, J.N., et al. (2024). Single-cell analysis of psoriasis resolution demonstrates an
783 inflammatory fibroblast state targeted by IL-23 blockade. Nat Commun *15*, 913.
784 https://doi.org/10.1038/s41467-024-44994-w.

785 61. Ma, F., Plazyo, O., Billi, A.C., Tsoi, L.C., Xing, X., Wasikowski, R., Gharaee-Kermani, M., Hile, G., Jiang, Y.,
786 Harms, P.W., et al. (2023). Single cell and spatial sequencing define processes by which keratinocytes and
787 fibroblasts amplify inflammatory responses in psoriasis. Nat Commun *14*, 3455.
788 https://doi.org/10.1038/s41467-023-39020-4.

789 62. Bragulla, H.H., and Homberger, D.G. (2009). Structure and functions of keratin proteins in simple,
790 stratified, keratinized and cornified epithelia. J Anat *214*, 516–559. https://doi.org/10.1111/j.1469-
791 7580.2009.01066.x.

792 63. Wang, J., Wang, C., Liu, L., Hong, S., Ru, Y., Sun, X., Chen, J., Zhang, M., Lin, N., Li, B., et al. (2023).
793 Adverse events associated with anti-IL-17 agents for psoriasis and psoriatic arthritis: a systematic scoping
794 review. Front Immunol *14*, 993057. https://doi.org/10.3389/fimmu.2023.993057.

795 64. Bieber, T. (2020). Interleukin-13: Targeting an underestimated cytokine in atopic dermatitis. Allergy *75*,
796 54–62. https://doi.org/10.1111/all.13954.

797 65. Gordon, K.B., Blauvelt, A., Papp, K.A., Langley, R.G., Luger, T., Ohtsuki, M., Reich, K., Amato, D., Ball,
798 S.G., Braun, D.K., et al. (2016). Phase 3 Trials of Ixekizumab in Moderate-to-Severe Plaque Psoriasis. N Engl J
799 Med *375*, 345–356. https://doi.org/10.1056/NEJMoa1512711.

800 66. Damiani, G., Conic, R.R.Z., de Vita, V., Costanzo, A., Regazzini, R., Pigatto, P.D.M., Bragazzi, N.L., Pacifico,
801 A., and Malagoli, P. (2019). When IL-17 inhibitors fail: Real-life evidence to switch from secukinumab to
802 adalimumab or ustekinumab. Dermatol Ther *32*, e12793. https://doi.org/10.1111/dth.12793.

803 67. Megna, M., Ruggiero, A., Martora, F., Vallone, Y., Guerrasio, G., and Potestio, L. (2024). Long-Term
804 Efficacy and Safety of Guselkumab in Psoriasis Patients Who Failed Anti-IL17: A Two-Year Real-Life Study. J
805 Clin Med *13*, 2691. https://doi.org/10.3390/jcm13092691.

806 68. Simpson, E.L., Bieber, T., Guttman-Yassky, E., Beck, L.A., Blauvelt, A., Cork, M.J., Silverberg, J.I.,
807 Deleuran, M., Kataoka, Y., Lacour, J.-P., et al. (2016). Two Phase 3 Trials of Dupilumab versus Placebo in
808 Atopic Dermatitis. N Engl J Med *375*, 2335–2348. https://doi.org/10.1056/NEJMoa1610020.

809 69. Wu, N.-L., Huang, D.-Y., Tsou, H.-N., Lin, Y.-C., and Lin, W.-W. (2015). Syk mediates IL-17-induced CCL20
810 expression by targeting Act1-dependent K63-linked ubiquitination of TRAF6. J Invest Dermatol *135*, 490–
811 498. https://doi.org/10.1038/jid.2014.383.

812 70. Woodward Davis, A.S., Roozen, H.N., Dufort, M.J., DeBerg, H.A., Delaney, M.A., Mair, F., Erickson, J.R.,
813 Slichter, C.K., Berkson, J.D., Klock, A.M., et al. (2019). The human tissue-resident CCR5+ T cell compartment
814 maintains protective and functional properties during inflammation. Sci Transl Med *11*, eaaw8718.
815 https://doi.org/10.1126/scitranslmed.aaw8718.

816 71. Sgambelluri, F., Diani, M., Altomare, A., Frigerio, E., Drago, L., Granucci, F., Banfi, G., Altomare, G., and
817 Reali, E. (2016). A role for CCR5(+)CD4 T cells in cutaneous psoriasis and for CD103(+) CCR4(+) CD8 Teff cells
818 in the associated systemic inflammation. J Autoimmun *70*, 80–90.
819 https://doi.org/10.1016/j.jaut.2016.03.019.

820 72. Reich, K., Armstrong, A.W., Langley, R.G., Flavin, S., Randazzo, B., Li, S., Hsu, M.-C., Branigan, P., and
821 Blauvelt, A. (2019). Guselkumab versus secukinumab for the treatment of moderate-to-severe psoriasis

822 (ECLIPSE): results from a phase 3, randomised controlled trial. Lancet *394*, 831–839.
823 https://doi.org/10.1016/S0140-6736(19)31773-8.

824 73. Kamsteeg, M., Zeeuwen, P.L.J.M., de Jongh, G.J., Rodijk-Olthuis, D., Zeeuwen-Franssen, M.E.J., van Erp,
825 P.E.J., and Schalkwijk, J. (2007). Increased expression of carbonic anhydrase II (CA II) in lesional skin of
826 atopic dermatitis: regulation by Th2 cytokines. J Invest Dermatol *127*, 1786–1789.
827 https://doi.org/10.1038/sj.jid.5700752.

828 74. Rochman, M., Kartashov, A.V., Caldwell, J.M., Collins, M.H., Stucke, E.M., Kc, K., Sherrill, J.D., Herren, J.,
829 Barski, A., and Rothenberg, M.E. (2015). Neurotrophic tyrosine kinase receptor 1 is a direct transcriptional
830 and epigenetic target of IL-13 involved in allergic inflammation. Mucosal Immunol *8*, 785–798.
831 https://doi.org/10.1038/mi.2014.109.

832 75. Ogawa, K., Ito, M., Takeuchi, K., Nakada, A., Heishi, M., Suto, H., Mitsuishi, K., Sugita, Y., Ogawa, H., and
833 Ra, C. (2005). Tenascin-C is upregulated in the skin lesions of patients with atopic dermatitis. J Dermatol Sci
834 *40*, 35–41. https://doi.org/10.1016/j.jdermsci.2005.06.001.

835 76. Peng, S., Chen, M., Yin, M., and Feng, H. (2021). Identifying the Potential Therapeutic Targets for Atopic
836 Dermatitis Through the Immune Infiltration Analysis and Construction of a ceRNA Network. CCID *Volume*
837 *14*, 437–453. https://doi.org/10.2147/CCID.S310426.

838 77. Simpson, E.L., Schlievert, P.M., Yoshida, T., Lussier, S., Boguniewicz, M., Hata, T., Fuxench, Z., De
839 Benedetto, A., Ong, P.Y., Ko, J., et al. (2023). Rapid reduction in Staphylococcus aureus in atopic dermatitis
840 subjects following dupilumab treatment. J Allergy Clin Immunol *152*, 1179–1195.
841 https://doi.org/10.1016/j.jaci.2023.05.026.

842 78. Werner, G., Sanyal, A., Mirizio, E., Hutchins, T., Tabib, T., Lafyatis, R., Jacobe, H., and Torok, K.S. (2023).
843 Single-Cell Transcriptome Analysis Identifies Subclusters with Inflammatory Fibroblast Responses in
844 Localized Scleroderma. Int J Mol Sci *24*, 9796. https://doi.org/10.3390/ijms24129796.

845 79. Zhu, H., Luo, H., Skaug, B., Tabib, T., Li, Y.-N., Tao, Y., Matei, A.-E., Lyons, M.A., Schett, G., Lafyatis, R., et
846 al. (2024). Fibroblast Subpopulations in Systemic Sclerosis: Functional Implications of Individual
847 Subpopulations and Correlations with Clinical Features. J Invest Dermatol *144*, 1251-1261.e13.
848 https://doi.org/10.1016/j.jid.2023.09.288.

849 80. Ho, K.T., and Reveille, J.D. (2003). The clinical relevance of autoantibodies in scleroderma. Arthritis Res
850 Ther *5*, 80–93. https://doi.org/10.1186/ar628.

851 81. Bangert, C., Rindler, K., Krausgruber, T., Alkon, N., Thaler, F.M., Kurz, H., Ayub, T., Demirtas, D.,
852 Fortelny, N., Vorstandlechner, V., et al. (2021). Persistence of mature dendritic cells, TH2A, and Tc2 cells
853 characterize clinically resolved atopic dermatitis under IL-4Rα blockade. Sci Immunol *6*, eabe2749.
854 https://doi.org/10.1126/sciimmunol.abe2749.

855 82. Ritchie, M.E., Phipson, B., Wu, D., Hu, Y., Law, C.W., Shi, W., and Smyth, G.K. (2015). limma powers
856 differential expression analyses for RNA-sequencing and microarray studies. Nucleic Acids Res *43*, e47.
857 https://doi.org/10.1093/nar/gkv007.

858 83. Leek, J.T., Johnson, W.E., Parker, H.S., Jaffe, A.E., and Storey, J.D. (2012). The sva package for removing
859 batch effects and other unwanted variation in high-throughput experiments. Bioinformatics *28*, 882–883.
860 https://doi.org/10.1093/bioinformatics/bts034.

861 84. Chen, E.Y., Tan, C.M., Kou, Y., Duan, Q., Wang, Z., Meirelles, G.V., Clark, N.R., and Ma'ayan, A. (2013).
862 Enrichr: interactive and collaborative HTML5 gene list enrichment analysis tool. BMC Bioinformatics *14*,
863 128. https://doi.org/10.1186/1471-2105-14-128.

864 85. Milacic, M., Beavers, D., Conley, P., Gong, C., Gillespie, M., Griss, J., Haw, R., Jassal, B., Matthews, L.,
865 May, B., et al. (2024). The Reactome Pathway Knowledgebase 2024. Nucleic Acids Res *52*, D672–D678.
866 https://doi.org/10.1093/nar/gkad1025.

867 86. Sollis, E., Mosaku, A., Abid, A., Buniello, A., Cerezo, M., Gil, L., Groza, T., Güneş, O., Hall, P., Hayhurst, J.,
868 et al. (2023). The NHGRI-EBI GWAS Catalog: knowledgebase and deposition resource. Nucleic Acids Res *51*,
869 D977–D985. https://doi.org/10.1093/nar/gkac1010.

870 87. Hao, Y., Hao, S., Andersen-Nissen, E., Mauck, W.M., Zheng, S., Butler, A., Lee, M.J., Wilk, A.J., Darby, C.,
871 Zager, M., et al. (2021). Integrated analysis of multimodal single-cell data. Cell *184*, 3573-3587.e29.
872 https://doi.org/10.1016/j.cell.2021.04.048.

873 88. Domínguez Conde, C., Xu, C., Jarvis, L.B., Rainbow, D.B., Wells, S.B., Gomes, T., Howlett, S.K., Suchanek,
874 O., Polanski, K., King, H.W., et al. (2022). Cross-tissue immune cell analysis reveals tissue-specific features in
875 humans. Science *376*, eabl5197. https://doi.org/10.1126/science.abl5197.

876 89. Reynolds, G., Vegh, P., Fletcher, J., Poyner, E.F.M., Stephenson, E., Goh, I., Botting, R.A., Huang, N.,
877 Olabi, B., Dubois, A., et al. (2021). Developmental cell programs are co-opted in inflammatory skin disease.
878 Science *371*, eaba6500. https://doi.org/10.1126/science.aba6500.

879 90. Xu, C., Prete, M., Webb, S., Jardine, L., Stewart, B.J., Hoo, R., He, P., Meyer, K.B., and Teichmann, S.A.
880 (2023). Automatic cell-type harmonization and integration across Human Cell Atlas datasets. Cell *186*,
881 5876-5891.e20. https://doi.org/10.1016/j.cell.2023.11.026.

882 91. Tirosh, I., Izar, B., Prakadan, S.M., Wadsworth, M.H., Treacy, D., Trombetta, J.J., Rotem, A., Rodman, C.,
883 Lian, C., Murphy, G., et al. (2016). Dissecting the multicellular ecosystem of metastatic melanoma by single-
884 cell RNA-seq. Science *352*, 189–196. https://doi.org/10.1126/science.aad0501.

885